

1N-27  
5874  
p-49



# Materials Research for High Speed Civil Transport and Generic Hypersonics - Adhesive Durability

Mark R. Allen  
*Boeing Commercial Airplane Group, Seattle, Washington*

(NASA-CR-198193) MATERIALS  
RESEARCH FOR HIGH SPEED CIVIL  
TRANSPORT AND GENERIC HYPERSONICS:  
ADHESIVE DURABILITY Final Report  
(Boeing Commercial Airplane Co.)  
49 p

N96-11496

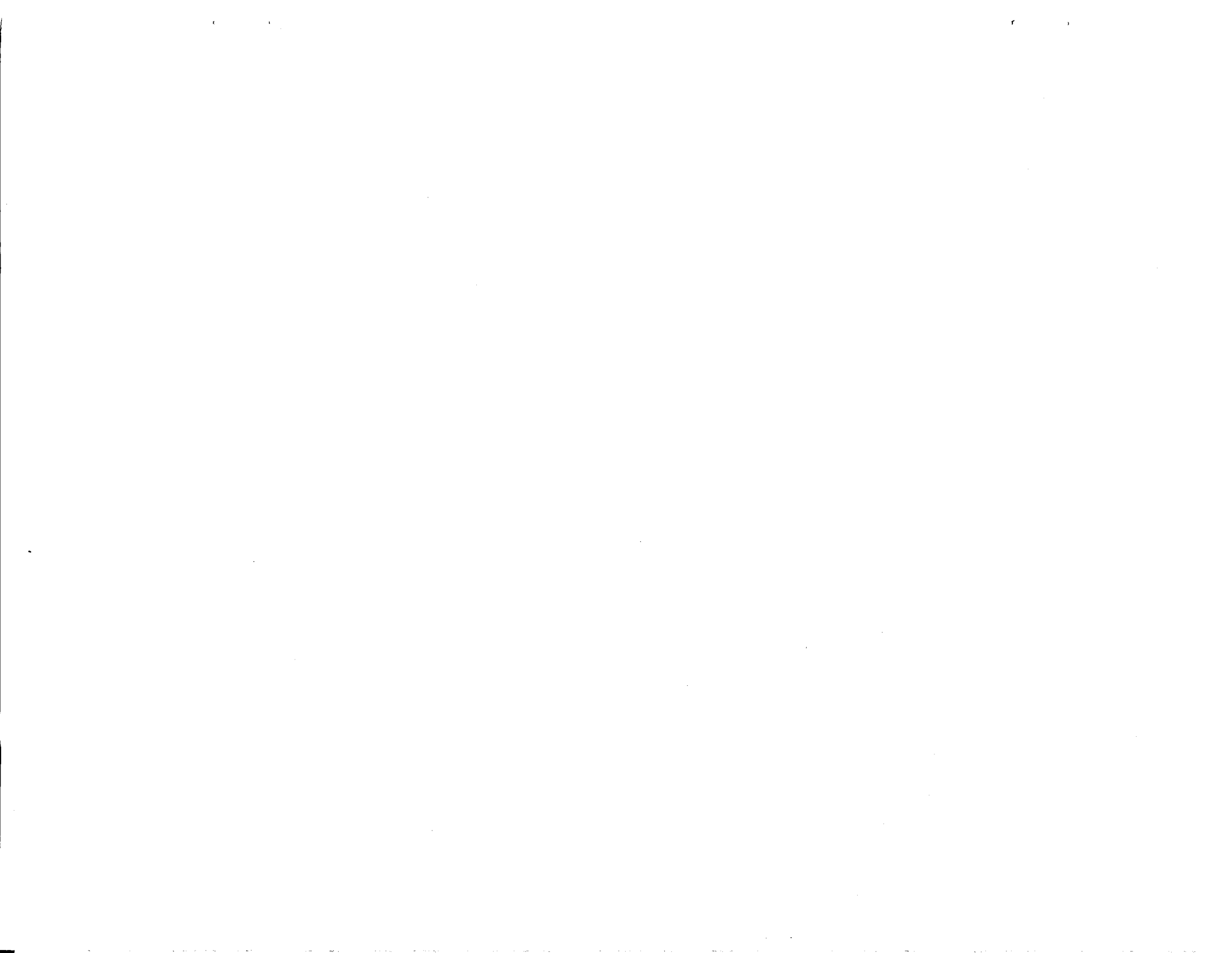
Unclas

G3/27 0068421

Contract NAS1-20013, Task 11

August 1995

National Aeronautics and  
Space Administration  
Langley Research Center  
Hampton, Virginia 23681-0001



## FOREWORD

The work described in this report was performed by the Boeing Commercial Airplane Group, Technology and Product Development, for the National Aeronautics and Space Administration (NASA), Langley Research Center (LaRC), under contract NAS1-20013. This contract was subdivided into multiple tasks, of which this effort was identified as Task 11, "Adhesive Durability." This report outlines the work performed developing and implementing a series of tests designed to study and characterize the long-term durability effects of thermal-mechanical fatigue on high-temperature adhesives for primary structural bonding applications. The NASA research task manager was assigned to Dr. W. Steven Johnson. His duties were reassigned to Mr. Edward T. Phillips after Dr. Johnson terminated his employment with NASA.

The performing organization within Boeing was the High-Speed Civil Transport (HSCT) Structures Group. Mr. Donald L. Grande was the program manager, Dr. Bjorn F. Backman and Dr. Matthew Miller were the structures technology supervisors, Mr. Peter G. Rimbos was the principal investigator, Mr. Daniel J. Hoffman was the task integrator and coordinator, and Mr. Mark R. Allen was the task leader. Additional contributions were made by the following personnel:

|                     |  |
|---------------------|--|
| Mr. Anthony Falcone | Specimen Fabrication and Test Leader                           |
| Ms. Erica D. Smith  | Specimen Fabrication and Test Integrator                       |
| Mr. Michael Walker  | Bonding Specialist   |
| Mr. Erich Freitas   | Bonding Specialist   |
| Mr. Brian Coxon     | Test Manager - Integrated Technologies (Intec)                 |
| Mr. Rod Wishart     | Test Analyst and Coordinator - Integrated Technologies (Intec) |



## TABLE OF CONTENTS

|  |    |
|--|----|
| List of Figures .....  | v  |
| Glossary .....   | vi |
| 1.0 Summary .....  | 1  |
| 2.0 Introduction .....   | 2  |
| 2.1 Objectives .....   | 2  |
| 2.2 Approach .....   | 2  |
| 3.0 Material Selection .....   | 6  |
| 4.0 Coupon Design .....  | 9  |
| 4.1 Candidate Test Specimens .....                                     | 9  |
| 4.2 Selected Test Specimens .....                                      | 12 |
| 5.0 Experimental Test Plan .....                                       | 15 |
| 6.0 Test Fixture Design .....  | 19 |
| 7.0 Specimen Fabrication and Bonding .....                             | 22 |
| 8.0 Conclusions .....  | 32 |
| 9.0 Recommendations .....  | 33 |
| 10.0 Bibliography .....  | 34 |
| Appendix A - Coupon Analysis Results .....                             | 35 |
| Appendix B - Titanium Coupon Measurements .....                        | 39 |
| Appendix C - Bonded Specimen Measurements .....                        | 40 |
| Appendix D - Ultimate-Strength Data for Thick-Adherend Specimens ..... | 42 |



## LIST OF FIGURES

|                |  |    |
|----------------|--|----|
| Figure 2.2-1.  | Cyclic Temperature Profile for Adhesive Durability Testing.....  | 3  |
| Figure 2.2-2.  | Different Approaches To Estimate Structural Responses .....  | 4  |
| Figure 3.0-1.  | HSCT Candidate Materials and Some Identified Characteristics .....   | 7  |
| Figure 4.1-1.  | HSCT Candidate Honeycomb Splice Joint.....   | 9  |
| Figure 4.1-2.  | Configuration Effects on Bonded Joint Failure Modes (NASA CR-<br>112235) .....                               | 10 |
| Figure 4.1-3.  | Thick-Adherend Specimen .....  | 10 |
| Figure 4.1-4.  | Free-Body Diagram for Selected Joints Showing Peel and Shear Forces .....                                    | 11 |
| Figure 4.1-5.  | Typical Shear-Stress Distribution Across Bonded Joints .....   | 11 |
| Figure 4.1-6.  | Analytical Model Used To Assess Load Transfer Across Bondline .....  | 12 |
| Figure 4.2-1.  | Thick-Adherend Coupon Specifications.....  | 13 |
| Figure 4.2-2.  | Estimated Lamina Properties for IM7/K3B.....   | 14 |
| Figure 5.0-1.  | Adhesive Durability Test Summary.....  | 16 |
| Figure 5.0-2.  | Typical Stress-Strain Behavior of Adhesives (FM-300K Adhesive).....  | 18 |
| Figure 6.0-1.  | DiCTE Thermal Fixture With Tension Specimen .....  | 19 |
| Figure 7.0-1.  | Oven Cure Cycle for BR57 Primer .....  | 22 |
| Figure 7.0-2.  | Oven Cure Cycle for R1-16 Primer.....  | 23 |
| Figure 7.0-3.  | Bonding Fixture for Five Thick-Adherend Specimens .....  | 23 |
| Figure 7.0-4.  | Autoclave Cure Cycle for FM 57.....  | 24 |
| Figure 7.0-5.  | Autoclave Cure Cycle for K3A.....  | 24 |
| Figure 7.0-6.  | TTU Scan of 12- by 12-in, 100-ply, IM7/K3B Laminate.....   | 26 |
| Figure 7.0-7.  | Measured Thicknesses on 12- by 12-in, 100-ply, IM7/K3B Laminate .....  | 26 |
| Figure 7.0-8.  | Condition of Laminate After Normal Bonding Process .....   | 27 |
| Figure 7.0-9.  | Prefabricated Notch in Laminate Using Metal Insert.....  | 28 |
| Figure 7.0-10. | Preformed Thick-Adherend Laminate Before Consolidation .....   | 29 |
| Figure 7.0-11. | Proposed Flatwise Tension Specimen for Thermal Fixture Testing.....  | 31 |
| Figure A-1.    | Variation of Load Transfer Through a Bonded Joint Using Soft,<br>Nominal, and Stiff Modulus Adhesives .....  | 35 |
| Figure A-2.    | Variation of Load Transfer Through a Bonded Joint With Identical and<br>Dissimilar Adherend Stiffnesses..... | 36 |
| Figure A-3.    | Effects of Adherend Tapering on Shear Load Transfer Across Bondlines.....                                    | 37 |
| Figure A-4.    | Thick-Adherend Specimen With Tapered Joints .....  | 38 |
| Figure B-1.    | Measurements From 25 Randomly Selected Titanium Coupons .....  | 39 |
| Figure C-1.    | Measurements of Specimens Bonded With K3A.....   | 40 |
| Figure C-2.    | Measurements of Specimens Bonded With FM 57 .....  | 41 |
| Figure D-1.    | Ultimate-Strength Data From Thick-Adherend Specimens With K3A<br>Adhesive .....                              | 42 |
| Figure D-2.    | Ultimate-Strength Data From Thick-Adherend Specimens With FM 57<br>Adhesive .....                            | 43 |

## GLOSSARY

|                |   |
|----------------|---|
| ATP            | advanced tow placement                        |
| CTE            | coefficient of thermal expansion              |
| DiCTE          | differential coefficient of thermal expansion |
| E              | modulus of elasticity                         |
| GAG            | ground-air-ground                             |
| HSCT           | High-Speed Civil Transport                    |
| HSR            | High-Speed Research                           |
| K <sub>c</sub> | plane stress fracture toughness               |
| msi            | million pounds force per square inch          |
| NASA           | National Aeronautics and Space Administration |
| NDI            | nondestructive inspection                     |
| PMC            | polymer matrix composite                      |
| RT             | room temperature                              |
| SPF            | superplastic forming                          |
| TTU            | through-transmission ultrasonic               |

## 1.0 SUMMARY

Several of the most promising structural concepts for the HSCT involve primary structural bonding. These range from using adhesives as a replacement for mechanical fasteners, thereby reducing part count and associated cost, to very lightweight honeycomb sandwich panels using polymer matrix composite (PMC) facesheets with titanium core.

Relatively little is known about the long-term durability of candidate HSCT adhesives subjected to mechanical loads in the relatively harsh supersonic operating environment. To date, bonding has been used primarily in lightly loaded secondary structure on subsonic aircraft. Epoxy adhesives are normally used for these applications, but they do not possess the high-temperature capability required for supersonic flight. This program was designed to initiate an understanding of the behavior of candidate HSCT materials when subjected to combined mechanical and thermal loads.

An experimental program was developed. It used shear and flatwise tension specimens to encompass the complex stress state that exists in typical bonded joints. The plan called for exposing both types of specimens to thermal cycling (room temperature (RT) to 300°F) for times up to 18 months. In some cases, mechanical load was applied through the use of hydraulics. In other cases, the specimens were placed in thermally actuated fixtures. These fixtures provided an inphase load because of differential thermal expansion of the specimen and various fixture components.

The initial test matrix used two adhesives (K3A and FM 57) and two adherends (IM7/K3B polymeric composite and the titanium alloy Ti-6Al-4V). Problems encountered in fabricating the lapshear test specimens demonstrated the need for new and improved adhesives, particularly for second-stage bond operations.

Both selected adhesives had recommended processing temperatures that were above the glass transition temperature of the K3B composite adherends. The adhesive cure cycle produced deformed adherends despite attempts at holding them in place. Also, one of the adhesives (K3A) displayed static strengths below what had been expected. Specimens using this adhesive will not enter durability testing until this strength issue is resolved.

The need is acute for an adhesive to secondarily bond PMC adherends or, alternatively, PMCs that remain stable at the processing temperatures of today's adhesives. Several promising structural concepts require the ability to secondarily bond.

Acceptable specimens using FM 57 adhesive and titanium adherends were fabricated and prepared for test in environmental chambers at Integrated Technologies, Inc. (Intec) of Bothell, Washington. Environmental cycling and durability testing will be conducted and reported under NASA Contract NAS1-20220, Task Assignment 15.

## 2.0 INTRODUCTION

### 2.1 Objectives

This program was established to initiate an understanding of the behavior of adhesives subjected to mechanical and thermal cycling for long periods of time. Prior use of adhesives has mostly been limited to lightly loaded secondary structure. These applications do not require a rigorous characterization of the adhesive material system. The high manufacturing costs associated with mechanically fastening structure has promoted a strong interest in advancing the use and application of adhesives to primary structure. Although many characteristics of adhesives are known, very little is understood regarding the combined long-term effects of cyclic testing at elevated temperature and load. This is particularly true for the high-temperature material classes being considered for use on the HSCT. Thus, expanding our knowledge on cyclic effects was identified as a primary objective of the adhesive durability task.

In addition, the relationships between long- and short-term performance were deemed important for two reasons. Testing after a relatively short period of time might identify adverse behavior, thereby permitting the discontinuation of further costly and superfluous testing on a material that is not durable in the HSCT environment. Periodic testing also allows assessment of deterioration rates for predicting extended behavior for the tested adhesive and, hopefully, for other candidate materials in the same material class. This allows consideration of newer candidate adhesives that may have improved properties or lower cost.

Before adhesive selections can be made for the HSCT, many different variations must be tested to ensure maximum safety and durability. A search to find simple relationships for complex conditions was therefore a goal of this task. Reliable but cost-effective test methods that are indicative of long-term performance are needed to reduce the time and expense necessary to narrow the focus to a few choices. Another objective of the test program was to consider and implement low-cost test methods. Flexibility in the test conditions allowed this to be achievable. In particular, by not precisely defining the load cycle to match real cyclic flight conditions, significant savings were realized. An innovative test fixture was selected to induce mechanical loads during the thermal cycle. It had some limitations but none that would substantially affect test expectations.

The final objective was to accumulate data to formulate degradation failure models for adhesives. These models would relate the different parameters and their influence on long-term strength degradation. Performance comparisons between specimens thermally and structurally cycled were to be made with specimens that were structurally cycled at RT and with specimens that were thermally cycled without load. Data from other sources would also be examined that show effects from uniform temperature and load exposures. In this way, the primary factors affecting degradation could be identified.

### 2.2 Approach

Because of the variety of loads, temperatures, and cyclic conditions to which an adhesive system could be subjected, a large number of tests would be required to fully map the material's useful envelope. Because this is not feasible, it was decided that the most basic conditions would be

evaluated at a cyclic schedule and temperature profile that would be representative of the HSCT. This profile is shown in figure 2.2-1.

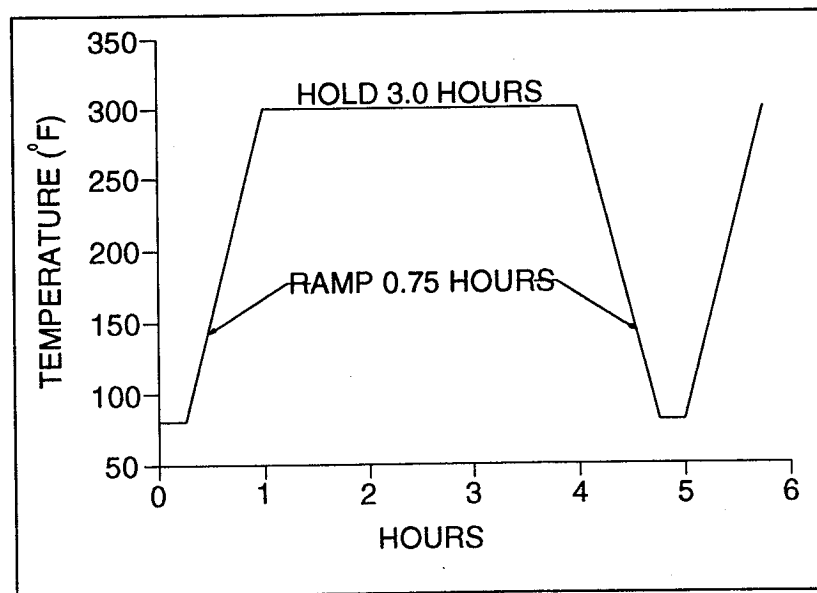


Figure 2.2-1. Cyclic Temperature Profile for Adhesive Durability Testing

The maximum service temperature is shown as 300°F. Some components on a mach 2.4 HSCT may see higher temperatures, but there are no plans to use adhesives in these areas. No currently available adhesive appears capable of achieving use temperatures above 300°F for long periods of time. The 300°F temperature selected for this program was considered achievable and sufficiently high to induce significant thermal effects.

Adhesively bonded joints are typically designed to transfer loads across the joint through a shearing action. In addition to the shear, virtually all joints develop a peeling load normal to the bonded surface. This undesirable tension load, created by load eccentricities, tries to pry the bonded joint apart. These eccentricities are omnipresent in standard joint designs and are quite unavoidable. The amount of peeling load can vary significantly, depending on the joint design and applied load. Typical values range between 20% and 60% of the applied shear load.

From an engineering and cost perspective, it is more effective to characterize the effects of shear and peel separately and then combine them with an interaction formula. The converse is to test to a point design and then extrapolate for other conditions. These two distinct approaches are shown in figure 2.2-2. Testing for shear and tension separately has the advantage of establishing the pure failure modes and significantly reducing the number of tests required to characterize the failure envelope. Some inaccuracies can be expected when interpolating combined shear- and peel-loading effects, but reasonable failure estimates can be obtained and interpolating is normally more accurate than extrapolating. For these reasons, tests were limited to evaluating adhesively bonded joints in a separate series of pure shear and peel load applications.

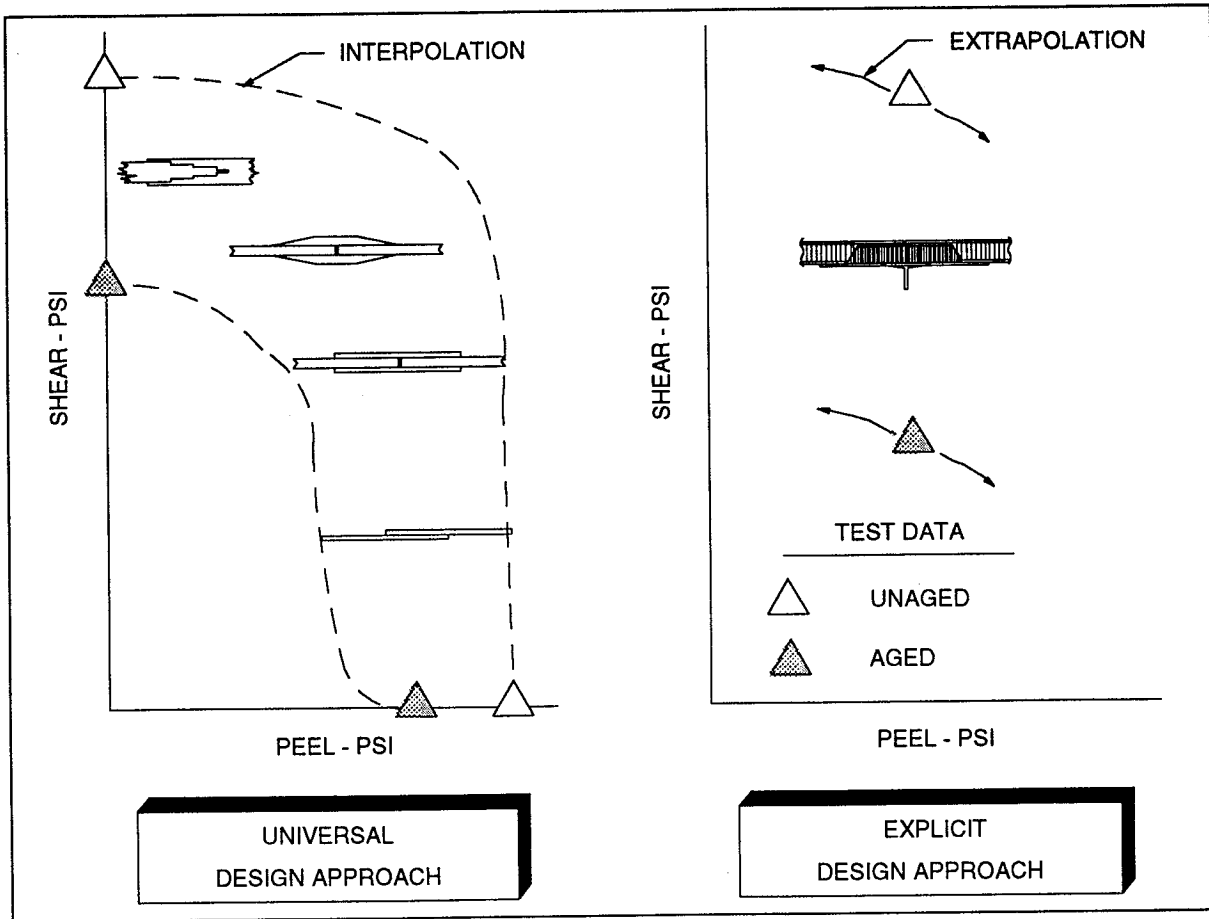


Figure 2.2-2. Different Approaches To Estimate Structural Responses

Specific ground-air-ground (GAG) load cycles that HSCT structural bonds might be required to withstand have been estimated. This complicated spectrum was not used on this program for several reasons. First, these loads are preliminary and probably will change with time. Because the fundamental degradation effects from aging under cyclic load and temperature were not yet known, it was felt that complex loading would inhibit understanding. In addition, the adhesives that will be used on HSCT have not been identified nor are their polymer families (epoxy, bismaleimide, thermoplastic) known. The added cost incurred by testing to very specific conditions is not justified because the long-term effects can vary from family to family. The intent of this test series was to broadly ascertain if these parameter combinations were synergistic, antagonistic, or inconsequential to long-term durability. It was further intended to establish not only a trend behavior for each system tested but to identify similarities between the different material systems tested.

Although long-term, real-time testing of adhesives will be required eventually, testing in this program was limited to approximately 13,000 hr (18 months). The high costs for a full life-cycle test (approximately 7-year duration) were not warranted on adhesive systems not positively identified for HSCT applications. The major durability issues with adhesives, as well as the behavioral relationships described above, should become evident within the planned test duration.

In addition to the adhesive material, the durability performance of adhesives can be influenced by the materials being bonded (adherends), as well as the surface preparation and priming of those materials. Two adherends and two adhesives were selected to explore this interaction relationship. No effort, however, was dedicated to investigating surface preparations or primers; the intent was to use established procedures. Successful bonding experience was a prerequisite for the selection of each process.

### 3.0 MATERIAL SELECTION

Promising structural concepts for the HSCT use a variety of materials. As part of the ongoing HSCT investigation, materials, including metals, PMCs, adhesives, and others, are being developed or refined to meet the needs of the program. As a result, properties of the various existing candidate materials are under continual development to improve selective deficiencies. Also, newer materials become candidates as they mature from the lab to commercially available products. Because of the many factors that affect material selection, no single system can be considered a clear winner at this time. The HSCT program maintains a list of candidate materials that exhibit the most beneficial attributes. Figure 3.0-1 is a reduced list of candidate materials and some of their important properties at the time this task was instigated. This list was used to select the adhesives and adherend materials for durability testing.

Both metals and PMCs were considered viable candidates. Because of the high temperatures involved, only titanium was considered for the metallic adherends; aluminum alloy properties are inadequate for operations above 250°F. For the PMC material class, only high-temperature resistant resins were examined. The same considerations were applied to adhesives.

The materials selected for the adherends were titanium (standard-mill-annealed Ti-6Al-4V) and IM7/K3B composite. Numerous varieties of titanium were and are being developed. The more advanced titaniums were not selected for this program because proven surface preparation procedures were not yet available. Ti-6Al-4V is a well-established titanium with good bonding experience. Because surface preparation was not the focus of this study, anything that might induce adhesive failures (failures along the interface between the adhesive and the adherend surface) was avoided. The goal was to have only cohesive failures (failures of the adhesive between the bonded surfaces). Also, properties of the newer alloys are not sufficiently different from Ti-6Al-4V to invalidate test results.

Of the PMCs, only IM7/K3B was considered a viable material for durability testing. The other high-temperature candidates, although exhibiting some better characteristics, were too developmental, and hence premature, to be included in a long-term test program. K3B was available as a commercial product, considered to have high thermo-oxidative stability, and considered to be a valid "representative" material for the polyimide material class.

FM 57 and K3A were selected for the adhesives. Very few adhesives were suitable for this test program. Most adhesives were incapable of performing at high temperatures and the few that could, deteriorated rapidly. FM 57 was an adhesive that had been well characterized and had demonstrated some high-temperature resistance. It had been in use for many years.

K3A adhesive was selected because of its demonstrated behavior at elevated temperatures. K3A adhesive is very similar to the K3B matrix material and was known to chemically bond with K3B, allaying concerns as to whether the adhesive would bond to the adherends.

| Temp Range           | Material Type            | Family       | Materials of Merit  | Advantages   | Issues   |
|----------------------|--------------------------|--------------|---|--|--|
| 275°F<br>to<br>350°F | Titanium                 | Alpha + Beta | B-CEZ   | High strength; Kc; E   | Costly in sheet/foil<br>Costly in sheet/foil<br>New alloy; moderate strength<br>Moderate properties<br>Moderate properties<br>Availability; high-cost foil |
|                      |                          |              | Ti-6-2222   | High strength; Kc; E   |  |
|                      |                          |              | Ti-62S  | Good strength; Kc; very high E; low cost   |  |
|                      | Titanium                 | Beta         | Ti-10-2-3   | Good thick section material  | Lower E; higher density<br>Lower E; higher density<br>Lower E; higher density  |
|                      |                          |              | IMI-550   | Good thick section material; SPF   |  |
|                      |                          |              | SP 700  | Good corros resist; strength; Kc; excel SPF  |  |
|                      | Thermoset Composites     | Cross-linked | PETI-5  | Improved processability compared to K3B  | Developmental<br>Solvent sens; hot/wet prop; process; developmental<br>Thermal stability; volatiles  |
|                      |                          |              | K3B   | Thermal stability  |  |
|                      | Thermoplastic Composites | Amorphous    | RD 92-107   | Improved processability compared to K3B  | Solvent sens; hot/wet prop; process; shelf life<br>Prepreg quality; microcracking<br>Developmental   |
|                      |                          |              | K3B   | Balanced properties; thermal stability   |  |
| Adhesives            | Thermoset                | AURUM        | Properties & processing by way of ATP                                 | Difficult processability<br>Availability in large quantities; database<br>Unproven adhesive perf; avail in large quantities<br>Availability; unproven adhesive performance<br>Unproven process; availability; cost<br>Processability |  |
|                      |                          | IAX          | Improved processability compared to K3B                               |  |  |
|                      | Thermoplastic            | K3B          | Good process; solvent resist; high-temp prop                          |  |  |
|                      |                          | IAX          | Moderate processability; solvent resistant                            |  |  |
| Hybrid Laminate      | Ti Base                  | K3A          | Good process; solvent resist; high-temp prop                          | Developmental; cost; processability<br>Developmental; high cost; avail; processability   |  |
|                      |                          | TPI          | Balanced properties; thermal stability<br>High-temperature properties |  |  |
| Hybrid Laminate      | Ti Base                  | Ti-Gr        | Excel strength; E; good Kc & fatigue; low density                     | Developmental; high cost; avail; processability  |  |
|                      |                          | Ti-Bor       | Excel strength; E; good Kc & fatigue; low density                     |  |  |

Notes: ATP advanced tow placement      Kc plane stress fracture toughness  
E modulus of elasticity                      SPF superplastic forming

Figure 3.0-1. HSCT Candidate Materials and Some Identified Characteristics

The other adhesive choices, like the PMCs, had insufficiently matured to a state that would warrant their inclusion in a long-term durability program.

A secondary benefit with these two adhesives is that they represent two different material families. FM 57 is a monomeric condensation polyimide and K3A is a fully imidized polyimide thermoplastic.

## 4.0 COUPON DESIGN

### 4.1 Candidate Test Specimens

A typical structural concept for the HSCT includes honeycomb-sandwich construction with splice joints, as shown in figure 4.1-1. Although this configuration is representative, it is definitely not appropriate for an adhesive durability study. In addition to being very costly, this configuration produces an everchanging complex array of shear and peel stresses that distribute across the joint, making understanding difficult. Simpler joint configurations were therefore explored with a goal of isolating the shear and peel stresses in separate tests.

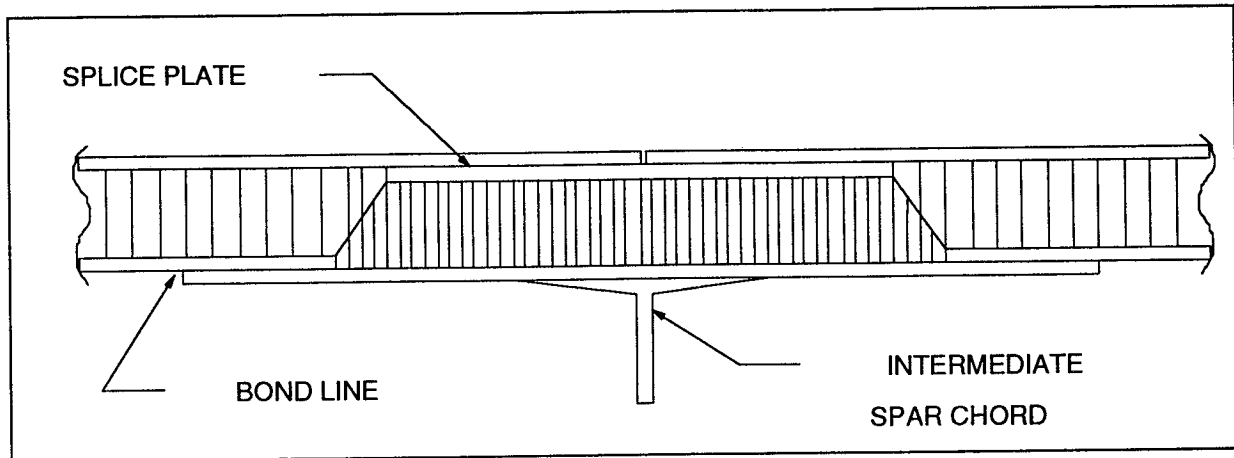


Figure 4.1-1. HSCT Candidate Honeycomb Splice Joint

The best test specimen and method for providing pure shear and minimum peel stresses on a bondline is known as the napkin ring test. This technique involves bonding two torsion tubes together and inducing uniform bondline shear through torsion or twisting loads applied to the ends of the specimen. Unfortunately, this method is very costly and requires a specialized load fixture to prevent any bending from being induced. It was not believed that a low-cost fixture could be developed that would fit the thermal chambers, resist the thermal cycling, and stay within the budget allotment. This method was therefore rejected.

Several different coupon constructions were evaluated for their adequacy to provide the desired load scheme. Figure 4.1-2 depicts common coupon joints and their normal failure modes. The more common designs for standard adhesive tests include single- and double-lap shear specimens. The more elaborate and efficient designs, particularly for critical applications, include other arrangements such as scarf joints or stepped lap joints.

Although the dominant failure mode in single- and double-lap shear specimens is peel, the other specimens in the figure also have significant contributions of peel, which lowers their overall "apparent" shear strength.

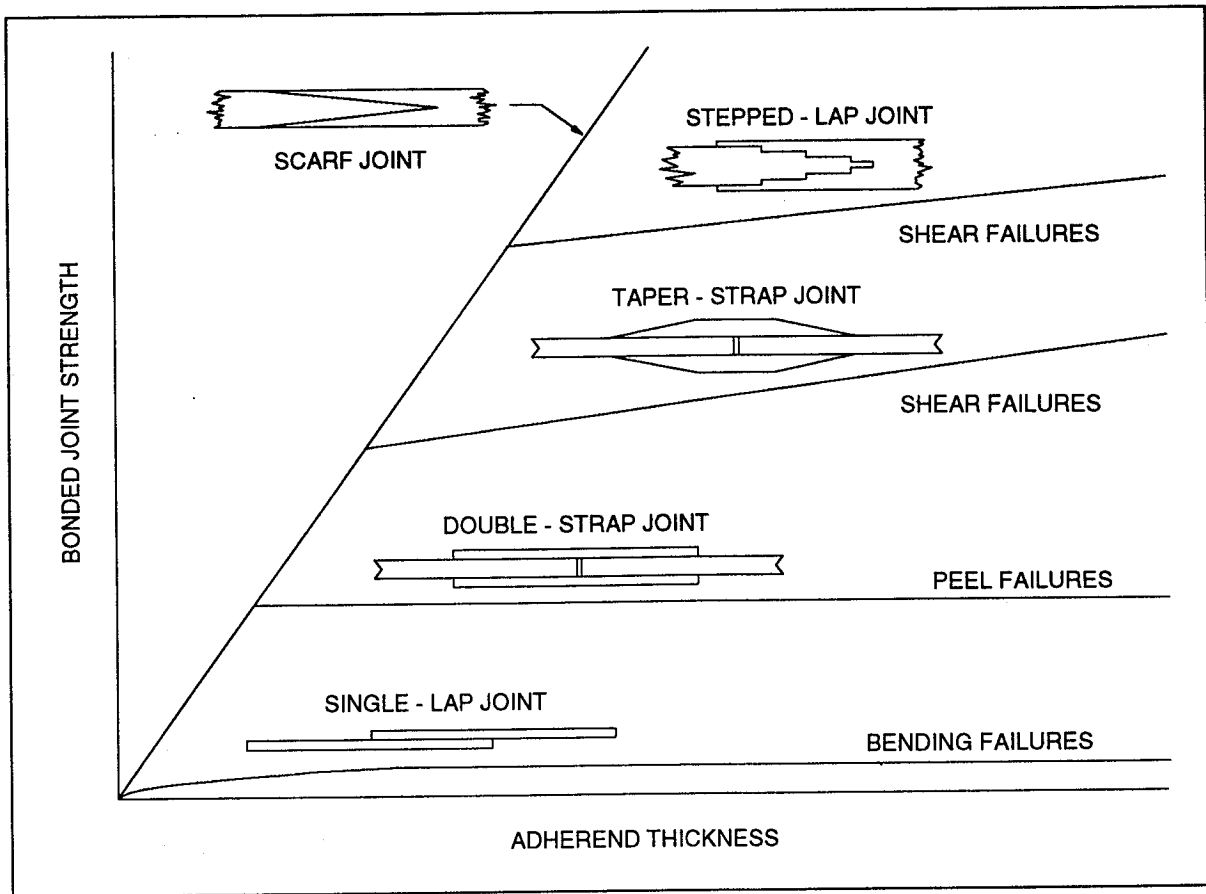


Figure 4.1-2. Configuration Effects on Bonded Joint Failure Modes (NASA CR-112235)

The specimen design that was selected for adhesive durability testing was based on a design that had been specially created and used for measuring shear stress and strain in adhesives. This specimen has adopted the name of *thick-adherend tensile-lap specimen*. It has been used in a procedure known as the KGR-1 test. Figure 4.1-3 shows the overall appearance of the thick-adherend specimen. The advantage of this specimen is that peel stresses are minimized because the center axis of the applied loads passes through the centerline of the bonded surface. This avoids inherent eccentricities commonly found in most other types of joints that generate these peel loads. Figure 4.1-4 shows the free-body diagram of loads for the two most common joints and for the thick-adherend specimen.

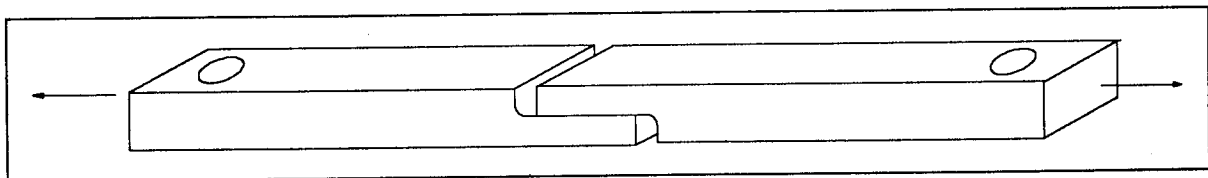


Figure 4.1-3. Thick-Adherend Specimen

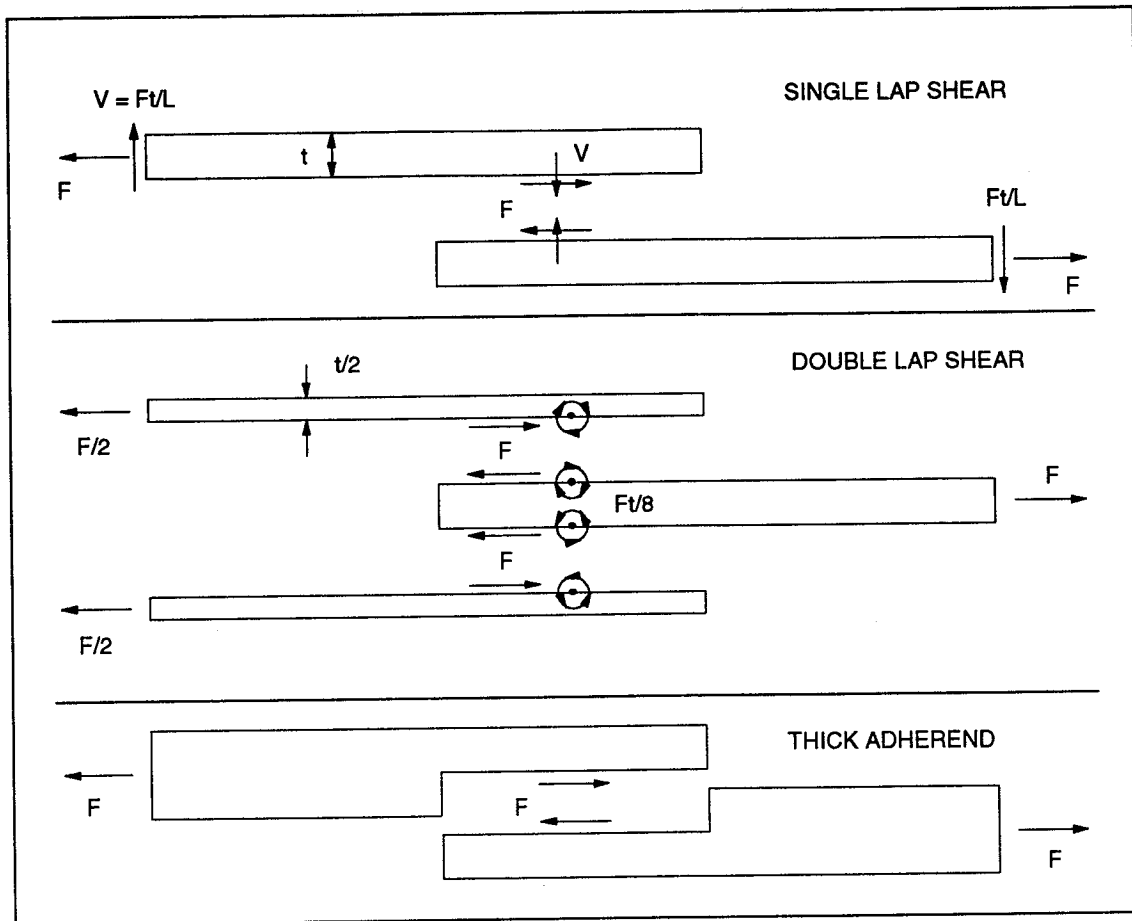


Figure 4.1-4. Free-Body Diagram for Selected Joints Showing Peel and Shear Forces

It is desirable to have a uniform or nearly uniform shear distribution along the length of the bondline. Without it, predictions and basic interpretations of adhesive performance become more complicated; uniformity clearly simplifies characterization efforts. Unfortunately, thick-adherend joints, similar to most other bonded joints, transfer a large portion of their load across the ends of the joint and transmit a relatively small portion across the center section. A symbolic representation of this behavior is shown in figure 4.1-5.

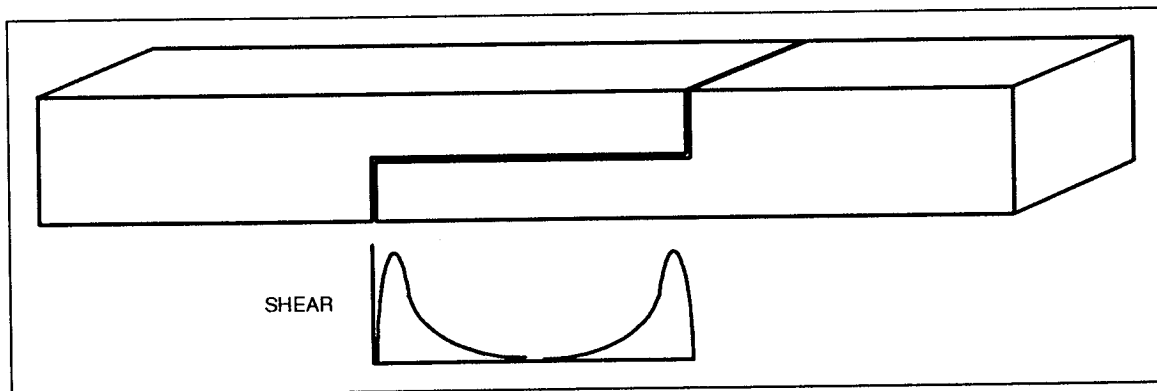


Figure 4.1-5. Typical Shear-Stress Distribution Across Bonded Joints

A low-effort study was performed to identify whether features could be employed that would produce a more nearly uniform stress distribution across the joint. A set of equations was derived that captured the axial and shear transfer loads in a single-lap shear joint. A unit load with the spring and element system, shown in figure 4.1-6, adequately modeled the essential parameters. The spring stiffnesses for both the adherends and the adhesive were controlled and varied by the modulus and thickness of the material.

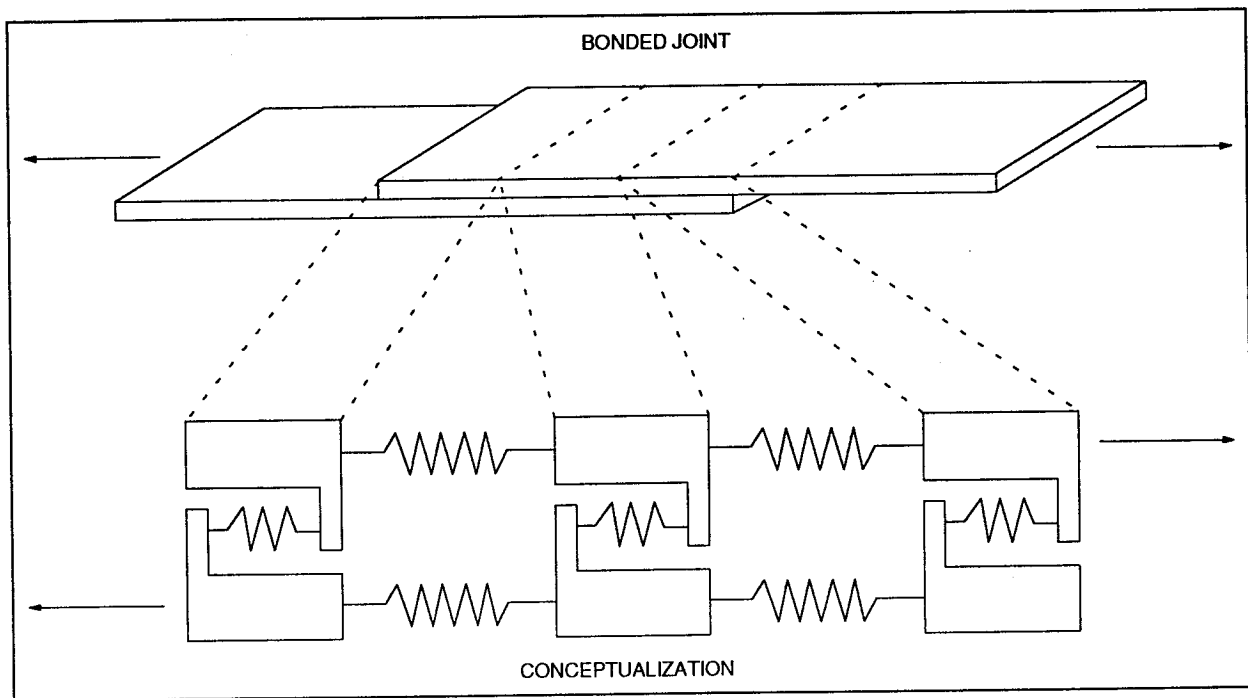


Figure 4.1-6. Analytical Model Used To Assess Load Transfer Across Bondline

Several different configurations were examined to observe their effects on load transfer. These included the relative differences between soft, nominal, and stiff adhesive moduli, different thicknesses between the upper and lower adherends, and different adherend tapering schemes.

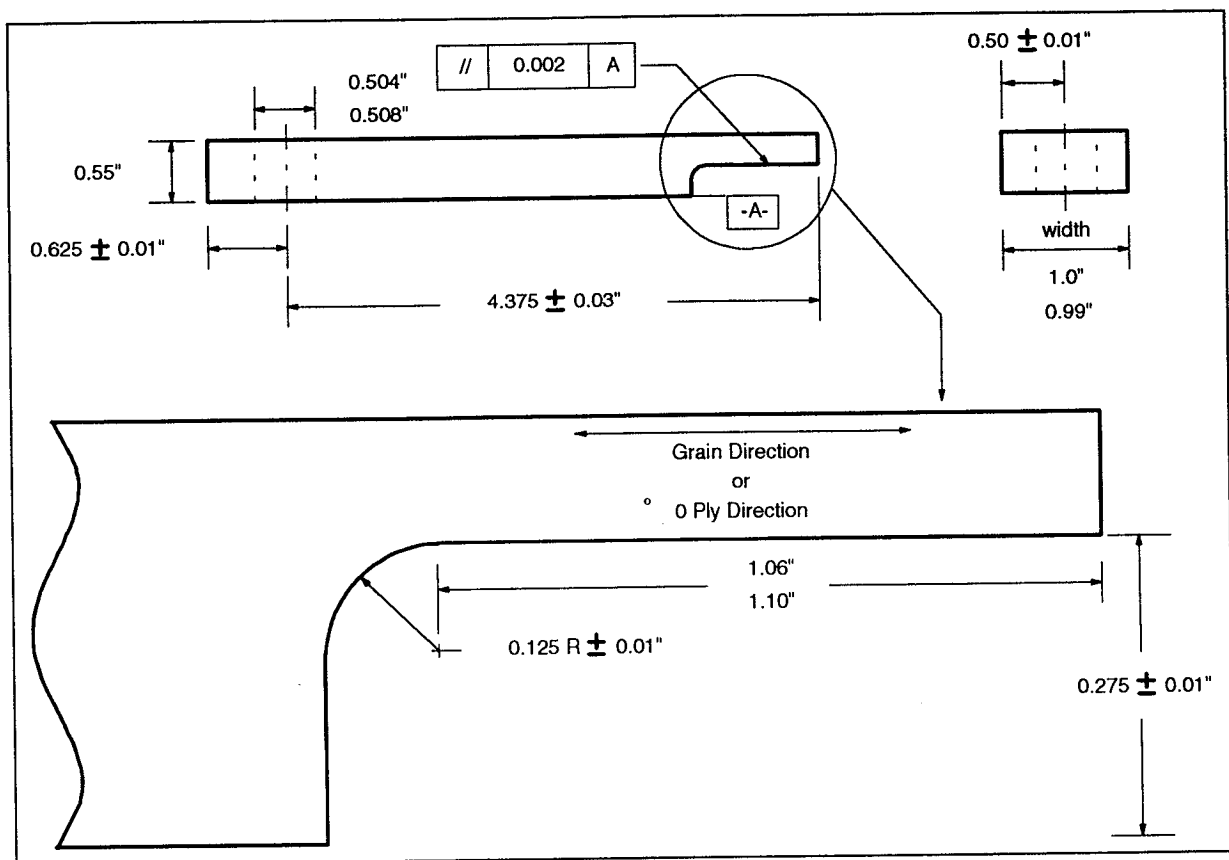
The results indicated that adhesive stiffness has a small but measurable effect on the stress distribution. Using adherends with different moduli provided similar results with most of the differences present at the ends of the lap. Tapering the adherends did provide a more uniform shear stress distribution but raised other concerns, particularly for the laminated composite specimens. Tapering the adherends would have produced unsymmetrical laminates, thereby giving them a tendency to warp and inducing peel stresses of unknown magnitude. While offering some potential for uniform stress distribution, it was felt that considerable development would be required to understand the peel stresses. It was concluded that using the more conventional thick-adherend lap specimen was the best approach for this task. Additional details can be found in appendix A.

## 4.2 Selected Test Specimens

Figure 4.2-1 gives the selected coupon dimensions. The length (9 in) was determined by the maximum allowable size that the load fixture would accommodate. The width (1 in) was set to

what traditionally has been determined to be the best compromise between economy and test-result influence. The bond overlap dimension (1 in) was also a compromise between economy and preferred behavior. A greater overlap would respond more closely to actual structure and would resist failure longer if the adhesive deteriorated during the long-term testing. Because a 0.5-in overlap is often satisfactorily used in adhesive testing, the 1-in overlap gave a reasonable cushion.

The thickness (0.55 in) was also a compromise. Thick-adherend specimens are normally 0.75 in thick to give proper rigidity, particularly through the notched end section, which must carry a significant bending moment. Normal thick-adherend specimens are made from aluminum and therefore have approximately two-thirds the stiffness of titanium. Because the 0.55-in specimens were made from titanium, their stiffness was actually greater than 0.75-in aluminum. Moreover, half of the specimens were to be made from laminated composites. The cost and difficulty of producing well-formed 0.75-in laminated specimens made them impractical. Even producing 0.55-in-thick laminates (100 plies) was considered a challenge.



Layup: [0/45/0<sub>2</sub>/-45/0<sub>2</sub>/90/0<sub>2</sub>/45/0<sub>2</sub>/-45/0<sub>2</sub>/90/0<sub>2</sub>/45/0<sub>3</sub>/-45/0]2s  
(composite adherends only)

Figure 4.2-1. Thick-Adherend Coupon Specifications

It was intended to expose the specimens in fixtures (see sec. 6.0) that were sensitive to the specimen's longitudinal modulus. Specimen loading was controlled by the thermal expansion of the fixture and the modulus of the specimens. The laminated coupons were therefore sized to have the same dimensions and longitudinal modulus as the titanium coupons. By matching stiffness, the

fixtures could be used for either type of specimen because the specimens would respond nearly identically regardless of the adherend composition (titanium or composite).

Designing both adherend types to have the same thermal expansion rather than identical moduli was rejected primarily for the loss of interchangeability of the load fixture between adherend types and the loss of a potentially significant contributor (thermal expansion) to long-term failure mechanisms between the two adherend types.

Ply orientations for the laminated adherends were established based on standard layup guidelines. At least 10% of 0s,  $\pm 45$ s, and 90s were included in the laminate. The stacking sequence was arranged so that no ply was placed at an angle greater than 45 deg from the preceding ply. No more than three identically oriented plies would be in succession. Symmetry was to be maintained about the center plane of the laminate as well as the quarter-thickness plane. The quarter-thickness plane of symmetry was included because the half-notched section at the end of each coupon required symmetry to uniformly transfer the axial and bending loads across the notch. The resulting layup was  $0_{68}/\pm 45_{12}/90_8$ , which gave a longitudinal modulus of approximately 15 msi. The specific layup sequence is given in figure 4.2-1. The total thickness of the laminate was approximately 0.58 in. This gave a near-equal stiffness (thickness times modulus) match with the titanium specimens ( $0.58 * 15E6 \cong 0.55 * 16E6$ ). Figure 4.2-2 lists IM7/K3B lamina property data used to predict laminate response. These data were obtained from several sources and extrapolated from laminate test data.

| Temperature | $E_x$ | $E_y$ | $\tau_{xy}$ | $\nu_{xy}$ | t      |
|-------------|-------|-------|-------------|------------|--------|
| RT          | 20.4  | 1.2   | 0.72        | 0.35       | 0.0058 |
| 300°F       | 20.4  | 0.85  | 0.51        | 0.37       | 0.0058 |
|             | msi   |       |             |            | inches |

Figure 4.2-2. Estimated Lamina Properties for IM7/K3B

One additional modification was made to the standard thick-adherend coupons to reduce the stress concentration in the notched section. As seen in figure 4.2-1, a 0.125-in radius was machined into each coupon. This was established by rounding the corner to the point that the peak corner load would never cause the factor of safety to be less than two for any load condition. The factor of safety was believed important to avoid cracking in the corner after extensive long-term testing had occurred. The laminated specimens were the most critical and determined the radius. Because the specimens were all to be identical, the titanium specimens were machined with the same radius, giving them a minimum factor of safety of approximately three.

## 5.0 EXPERIMENTAL TEST PLAN

The advantages of extending adhesive bonding to primary structure are well documented but its implications are not. Preliminary data suggest that adhesives can be successfully employed but the data are incomplete. Testing of adhesively bonded joints has almost exclusively been limited to single parameters, with little attention devoted to cyclic effects. Temperature and load studies, in particular, have concentrated on uniform test conditions. This has been justified because adhesives have rarely been used in primary structural applications or subjected to frequent or widely diverse environmental changes.

Neither the primary structural material nor the intended adhesives have been identified for the HSCT. While material selection is being considered, some basic issues about the general behavior of adhesives can be resolved. These include the interactions of multiple variables and their influence on long-term durability. This will be particularly important when developing test programs for selected adhesives. Demonstrating lifetime performance (60,000 hr) requires 7 years of testing. Intelligently streamlining the long-term test programs can dramatically reduce costs without sacrificing confidence in the detection of weaknesses or pitfalls. This can only occur if investigative testing is first performed. Parameter interactions that have been identified to have little influence on long-term performance can then be evaluated with a minimum of tests.

The experimental test plan for this study focused on three main elements: first and foremost was to determine the aging effects of strain (shear and tension) and temperature on strength degradation of adhesively bonded joints; secondly, to establish the threshold at which structural loading does not induce material degradation; and lastly, to provide a basis for simplifying analyses and subsequent long-term testing.

In order to understand how interactions affect responses, each condition must be evaluated separately and in combination. The test plan for adhesive durability conformed to this approach. There were four different test conditions planned: (1) baseline tests, (2) cyclic load tests at uniform temperature, (3) cyclic temperature tests without load, and (4) cyclic thermal-mechanical tests. The proposed lapshear test plan for each adhesive-adherend combination is shown in figure 5.0-1.

| Specimen Series Number | Type of Test              | Exposure Duration | Max Test Temp | Max Load | Replicates |
|------------------------|---------------------------|-------------------|---------------|----------|------------|
| 1                      | baseline                  | none              | RT            | failure  | 5          |
| 2                      | cyclic load               | 6 months          | RT            | 25%      | 1          |
| 3                      | cyclic load               | 6 months          | RT            | 50%      | 1          |
| 4                      | cyclic load               | 6 months          | RT            | 75%      | 1          |
| 5                      | cyclic load               | 6 months          | RT            | 100%     | 1          |
| 6                      | cyclic load               | 18 months         | RT            | 25%      | 1          |
| 7                      | cyclic load               | 18 months         | RT            | 50%      | 1          |
| 8                      | cyclic load               | 18 months         | RT            | 75%      | 1          |
| 9                      | cyclic load               | 18 months         | RT            | 100%     | 1          |
| 10                     | cyclic temperature        | 6 months          | 300°F         | 0%       | 3          |
| 11                     | cyclic temperature        | 18 months         | 300°F         | 0%       | 3          |
| 12                     | cyclic load & temperature | 6 months          | 300°F         | 25%      | 1          |
| 13                     | cyclic load & temperature | 6 months          | 300°F         | 50%      | 1          |
| 14                     | cyclic load & temperature | 6 months          | 300°F         | 75%      | 1          |
| 15                     | cyclic load & temperature | 6 months          | 300°F         | 100%     | 1          |
| 16                     | cyclic load & temperature | 18 months         | 300°F         | 25%      | 1          |
| 17                     | cyclic load & temperature | 18 months         | 300°F         | 50%      | 1          |
| 18                     | cyclic load & temperature | 18 months         | 300°F         | 75%      | 1          |

Figure 5.0-1. Adhesive Durability Test Summary

The maximum duration for testing was set to 18 months (13,000 hr). This would give a first look at how adhesives behave under combined thermal and structural loading. A shorter period, set at 6 months (4,300 hr) using identical test conditions, was also established to obtain more immediate results and to preview trends and tendencies for future work development. Most unanticipated reactions would likely be found within this period.

The unconditioned tests were to establish baseline ultimate strengths. The cyclic load testing at uniform temperature was planned at RT to isolate load effects at minimal costs. A similar test series, performed at a constant 300°F, would have made these tests more complete, but were not included because of cost constraints. The thermally cycled specimens without load would coexist in the same thermal chamber as the specimens that were being cyclically loaded. This isolates load and thermal effects from thermal effects alone at minimum costs, while ensuring that the other environmental conditions to be identical for these specimens. All cyclic testing was to follow the profile outlined in figure 2.2-1.

The expense of operating the thermal oven would have prevented all but a few tests from being performed. To enhance the task and secure a more efficient use of funding, it was decided to "piggyback" with the Composites Durability task, which was operating a thermal chamber at less than capacity. This allowed the number of tests to be expanded. Limitations still remained with the number of slots that were available in the chamber and the costs of fabricating, fixturing, and residual-strength testing specimens. As a result, usually only one specimen per condition was

planned for testing. Replications, although highly preferred, were simply unattainable. Because trends were the objective, it was believed that more diverse information could be obtained from single data points and variations could be estimated from all tests together. Because of the minimal costs associated with tests not involving cyclic loading, three replications were planned for each specimen type to give some indications of variation.

Fixture designs hinged on the load requirements of each specimen. Reasons for this are given in section 6.0, "Test Fixture Design." Therefore, maximum loads to be applied to each specimen were needed before the load fixtures could be designed and fabricated. Very little (and no direct) data were available that would establish the strengths of either FM 57 or K3A with thick-adherend lapshear specimens. Obtaining actual stress-strain test data for either FM 57 or K3A was not feasible. The specialized equipment necessary to obtain these data was not accessible for this task before fixture design needed to begin. Sufficient data were available to make reasonable estimates. Some test data, although bonded under a different process, indicated that K3A adhesives would fail at 3,750 psi at 350°F using a 0.5-in overlap on a single-lap shear specimen. Some data from FM 57 adhesive single-lap joint tests showed strengths of 3,100 psi at 350°F. Overall, the strengths appeared to be reasonably close to warrant identical load conditions.

Figure 5.0-2 shows the adhesive behavior of FM-300K at various temperatures. Although FM 57 and K3A adhesives would respond somewhat differently, the basic characteristics are expected to be representative. Specifically, there would be an initial linear portion of the stress-strain curve, followed by a nonlinear portion. This behavior is also typical of metallic materials. The wide variation in strengths seen for FM-300K over the broad range of temperatures would not be expected for either selected adhesive. Because these two adhesives are polyimides, they should retain most of their strength up to 300°F. They would also be expected to have a relatively sharp break between the linear and nonlinear portion of the stress-strain curve.

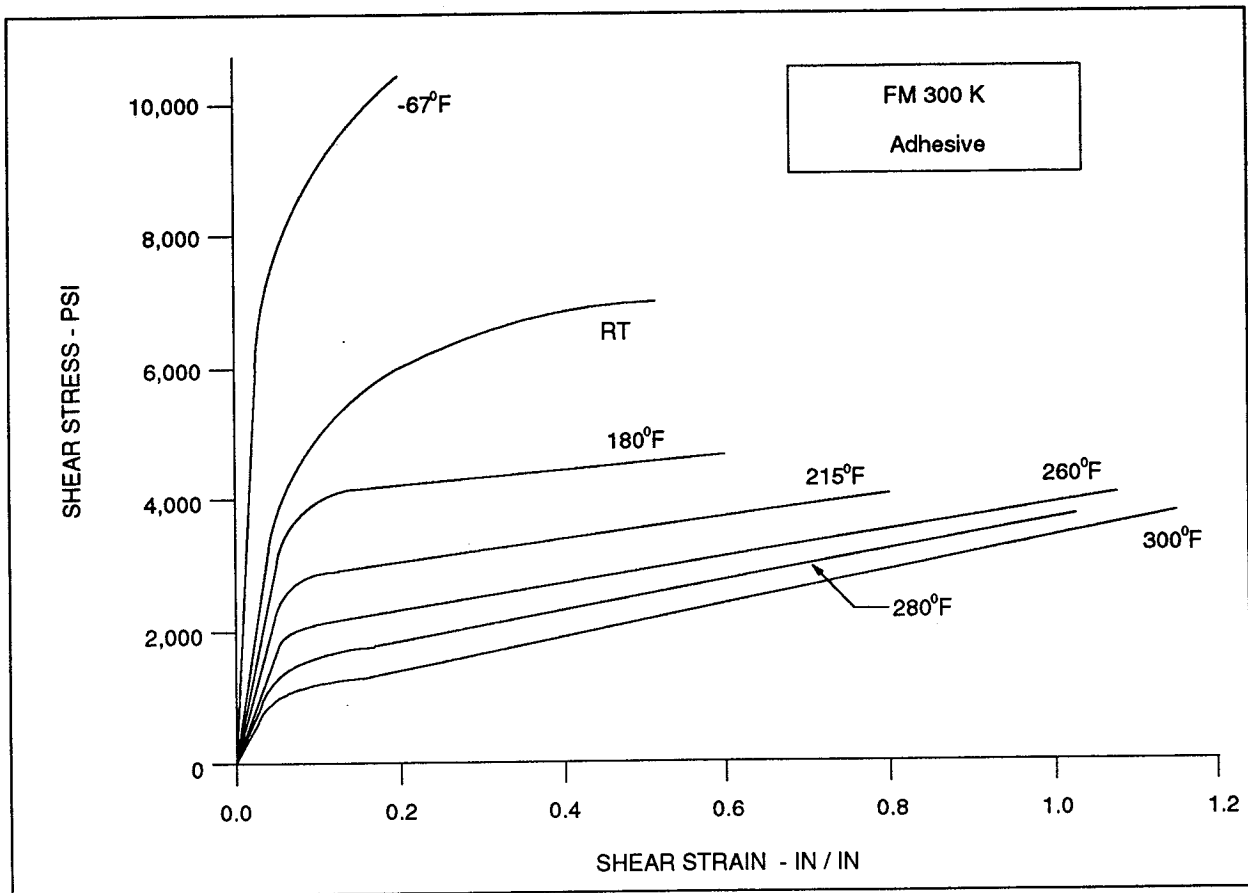


Figure 5.0-2. Typical Stress-Strain Behavior of Adhesives (FM-300K Adhesive)

Tests from other adhesives have demonstrated that loads operated well within the nonlinear region of the stress-strain curve significantly reduce the durability of the material. Because the behavior of neither adhesive was known, it was not possible to target a specific peak load for each cycle.

It was realized that durability may be significantly affected by the peak cyclic load. Therefore, a range of loads was assigned to help identify how loads affect durability and whether there is a threshold load level at which degradation does not occur, as seen in metallic materials. Four load levels were established. All were referenced to a single load. This reference load was set to 3,000 lb, the highest value considered obtainable for both adhesives to exhibit significant endurance. This was not a load that was expected to allow the specimens to endure the entire planned test period. Rather, it would provide a basis for collecting both short-term excursion experiences (i.e., occasional deviations from planned norms) and potential long-term residual capabilities. Four load cases were selected for study: 25%, 50%, 75%, and 100% of the reference load. These would be the maximum loads attained during each thermal cycle. The minimum cyclic loads would be zero.

All combinations of testing were to be identical, within cost limitations. The two adhesives (K3A and FM 57) and two adherend materials (titanium and IM7/K3B) gave four specimen combinations. This resulted in 104 planned lapshear tests.

## 6.0 TEST FIXTURE DESIGN

The myriad of tests required to validate any selected material system for a 60,000-hr life demands numerous ovens and test fixtures. The associated costs are substantial enough to warrant exploring more economical methods. To afford a reasonable number of tests for the adhesive durability task, techniques other than standard hydraulic load fixtures and single fixture ovens were also necessary.

One purpose of Task 10, "Composites Durability," a sister program, was to study alternative test methods. One development from that study was the differential coefficients of thermal expansion (DiCTE) fixture. This fixture takes advantage of the coefficient of thermal expansion (CTE) mismatch of two metals (invar and stainless steel) to provide displacement-controlled tension load cycles in phase with slow thermal cycling. An illustration of this fixture is shown in figure 6.0-1.

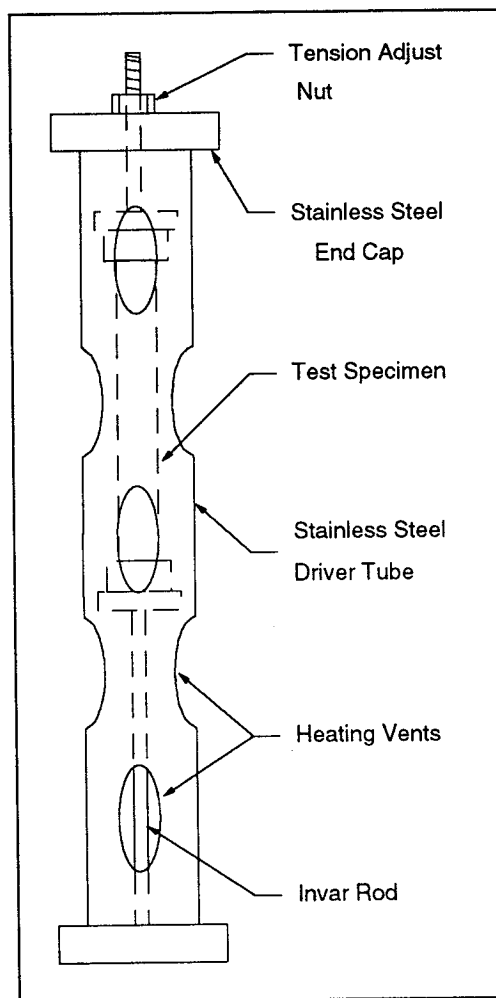


Figure 6.0-1. DiCTE Thermal Fixture With Tension Specimen

Actuation of the fixture relies on a simple mechanical principle. The stainless-steel driver has a much higher CTE than the invar-steel reaction rod ( $9.75 \mu\text{in}/^\circ\text{F}$  versus  $1.1 \mu\text{in}/^\circ\text{F}$ ). As temperatures increase, the driver expands and exerts a tensile force on the specimen, which is reacted by the relatively nonexpanding invar rod. The specimen is therefore strain controlled, with

load linearly dependent on specimen stiffness and environmental temperature. Maximum strains are controlled by the size of the fixture and its components. However, the fixture dimensions were limited by the chamber size but could nevertheless produce more than 0.004 in/in strains with a 280°F temperature variation. In most designs, the stiffness of the specimens is considerably softer than the steel components, so specimen influences on total strains are typically minor but were included in the fixture design. The length of the fixtures was approximately 18 in and the width was 3.5 in. This allowed for 25 fixtures to be mounted in the chamber.

The equation that determines specimen strain is—

$$\epsilon_S = \frac{\Delta T(C_S L_S - C_R L_R + C_D L_D)}{L_S + L_R \left( \frac{E_S A_S}{E_R A_R} \right) + L_D \left( \frac{E_S A_S}{E_D A_D} \right)}$$

Where:

- A = cross-sectional area
- C = coefficient of thermal expansion
- E = longitudinal modulus
- L = original length
- $\Delta T$  = temperature change

And subscripts:

- D = driver
- R = reaction rod
- S = specimen

An important consideration in the design of the fixture was its thermal mass. Heat transfer becomes consequential if cyclic times are required to be relatively short. The time necessary for the fixture to reach equilibrium is dependent on the ability of each component to absorb and dissipate heat rapidly. Maximizing surface areas and minimizing cross-sectional areas achieves this property. The stainless-steel tube (driver) was chosen because of its large surface area, thin wall thickness, and inherent alignment and stability advantages. The narrow invar reaction rod has a small cross-sectional area with high strength.

Trial tests of these thermal fixtures were conducted by Task 10 to identify unanticipated problems and to validate analyses. These tests have shown that fixture and specimen relaxation were insignificant for a 50-cycle test (3.5 hr/cycle). Readjustments, however, to compensate for any strain relief can easily be made through the tension adjustment nut between cycles. Strain predictions versus temperature came within 0.6% of actual recordings. The cost to manufacture these fixtures was slightly more than \$1,000/unit, a remarkably inexpensive load device.

Ordinarily, applied load would be monitored through strain-gage readings equated to equivalent load. For common small-coupon testing, these high-temperature gages can be attached to either the invar rod or to the coupon itself for strain response. Load-calibration tests can be conducted to chart their equivalence. Thick-adherend specimens preclude this technique. The unusually large thickness for coupons combined with the relatively high modulus of titanium gives a very high stiffness. The amount of strain necessary to produce the peak loads planned for the 25%, 50%,

75%, and 100% load cases, with this high a stiffness, equates to 85, 170, 260, and 340  $\mu\text{in}$ , respectively. These peak strains, and their intermediate values, fall within the noise level of strain gages. Therefore, reliable load (strain) data must be obtained through another mechanism.

Adding a load cell to the fixture was discarded because of added complexities and expense. The fixture would have to be designed to include the displacement of the load cell, the load cell would have to be temperature tolerant and thermally stable, and the additional costs would diminish the low-cost appeal. Efforts focused on retaining strain gages in areas of high stress concentrations. Several options were available, from placing strain gages in naturally occurring high-intensity stress areas, to artificially inducing stress concentrations into remote sections of the specimen or fixture. The selected option was to place a gage on the edge of the adherend, adjacent to the pin-loaded hole. The hole would be oversized to meet minimum edge-margin requirements. This would give a higher strain reading, relative to the strains across the joint itself. The strains would have to be calibrated to a load under a thermal cycle using a calibrated hydraulic load fixture.

## 7.0 SPECIMEN FABRICATION AND BONDING

Including planned excess, 104 titanium adherends and 98 composite (IM7/K3B) adherends were fabricated, to produce 52 titanium and 49 composite specimens. All titanium blanks were cut from the same 0.625-in-thick parent sheet (Mil-T-9046, annealed Ti-6AL-4V). The longitudinal coupon direction was aligned with the grain of the titanium. The titanium was milled to the planned 0.55-in thickness. Measured dimensions of some randomly selected finished coupons are given in appendix B. In most cases, coupon dimensions met specifications. When not, the error was within 3 mils. The need for high tolerances was to ensure that the bonded surfaces were parallel and within 2-mil waviness. This would help ensure a nearly uniform bond thickness. Specific influences on strength of varying bond thicknesses and average thicknesses greater than or less than the planned 5-mil thickness were not known for either adhesive, so thickness variations were minimized as much as possible.

All titanium adherends had a surface preparation of chromic acid anodize, in accordance with BAC 5890, using 5V. For bonding with the FM 57 adhesive, a primer (Cytac BR57) was applied. This primer was brush coated onto the adherends and flashed off and cured in accordance with figure 7.0-1. For bonding with K3A adhesive, a primer (DuPont R1-16 polyamide acid, NMP solution) was applied. This primer was brush coated onto the adherends and flashed off and cured in accordance with figure 7.0-2.

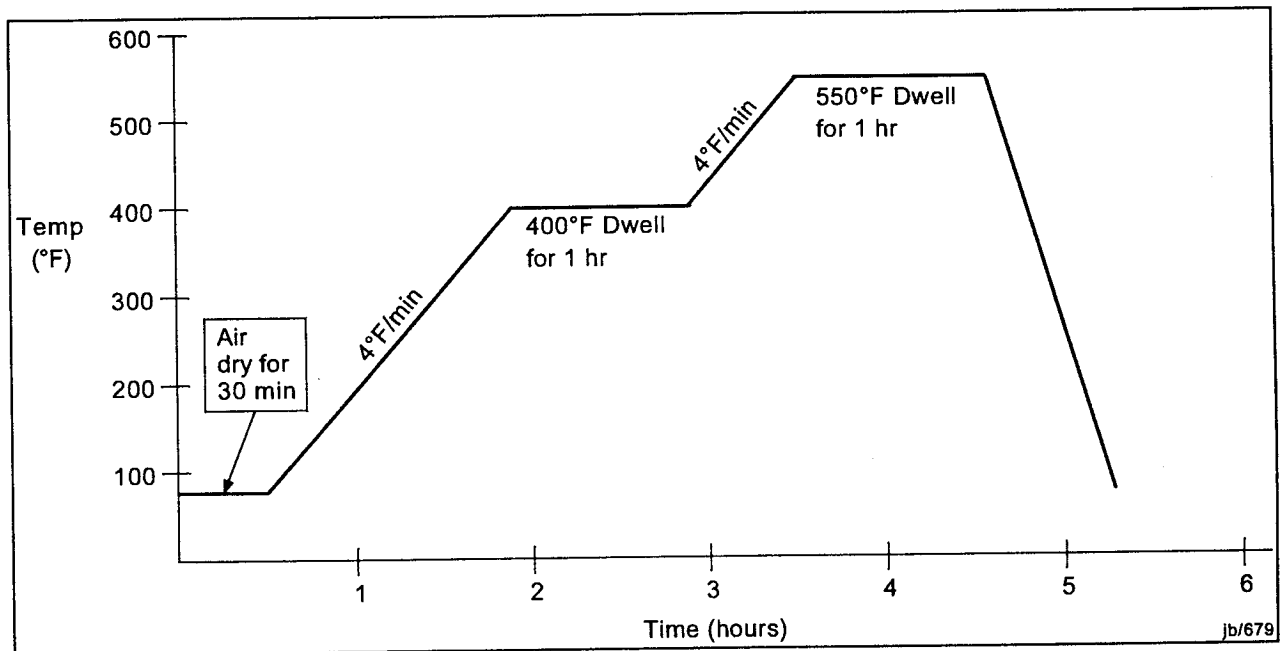


Figure 7.0-1. Oven Cure Cycle for BR57 Primer

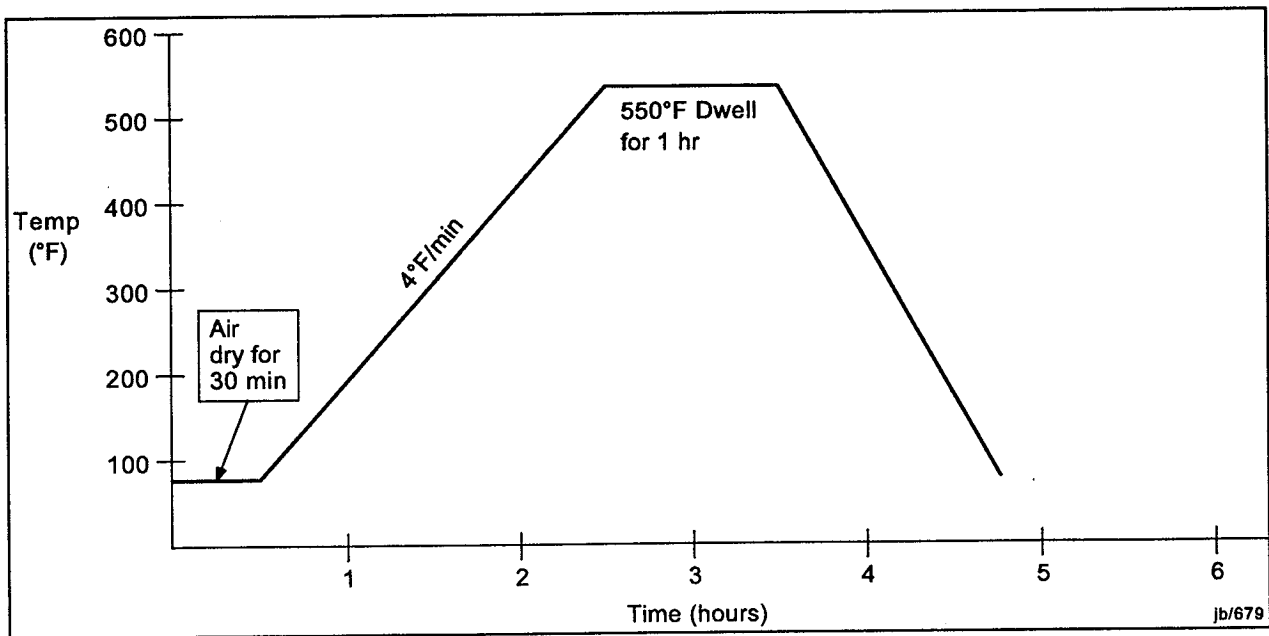
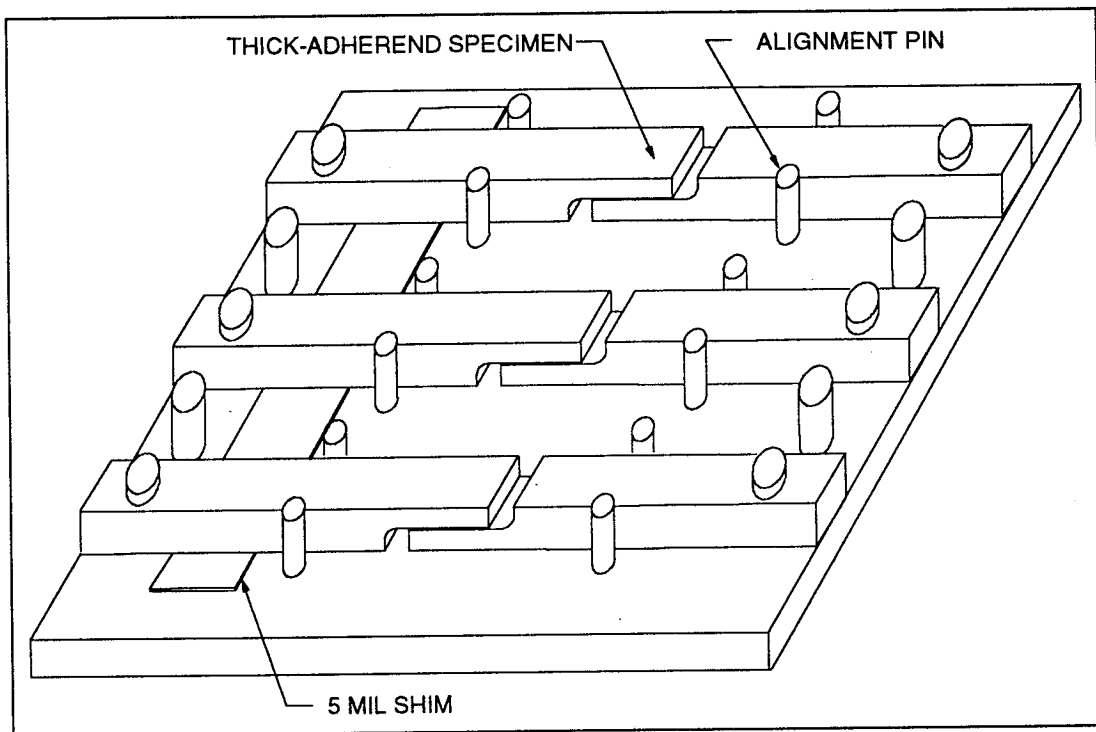


Figure 7.0-2. Oven Cure Cycle for R1-16 Primer

A special fixture for thick-adherend specimens was used to accomplish the bonding (fig. 7.0-3).



Note: For illustrative purposes, the fixture is shown with three specimens instead of five.

Figure 7.0-3. Bonding Fixture for Five Thick-Adherend Specimens

The fixture was intended to properly align the coupons and fix the bonding surface overlap dimension to 1 in. The shim was used to separate the upper and lower coupons by 5 mils, the desired bond thickness. This prevented the adhesive from being squeezed out by the bonding

pressure, which is applied during the bonding process to make positive contact. Before bonding the specimens, the fixture was coated with Frekote, a release agent. Adherends were then loaded into the fixture. The FM 57 specimens were cured in accordance with figure 7.0-4 and the K3A specimens in accordance with figure 7.0-5.

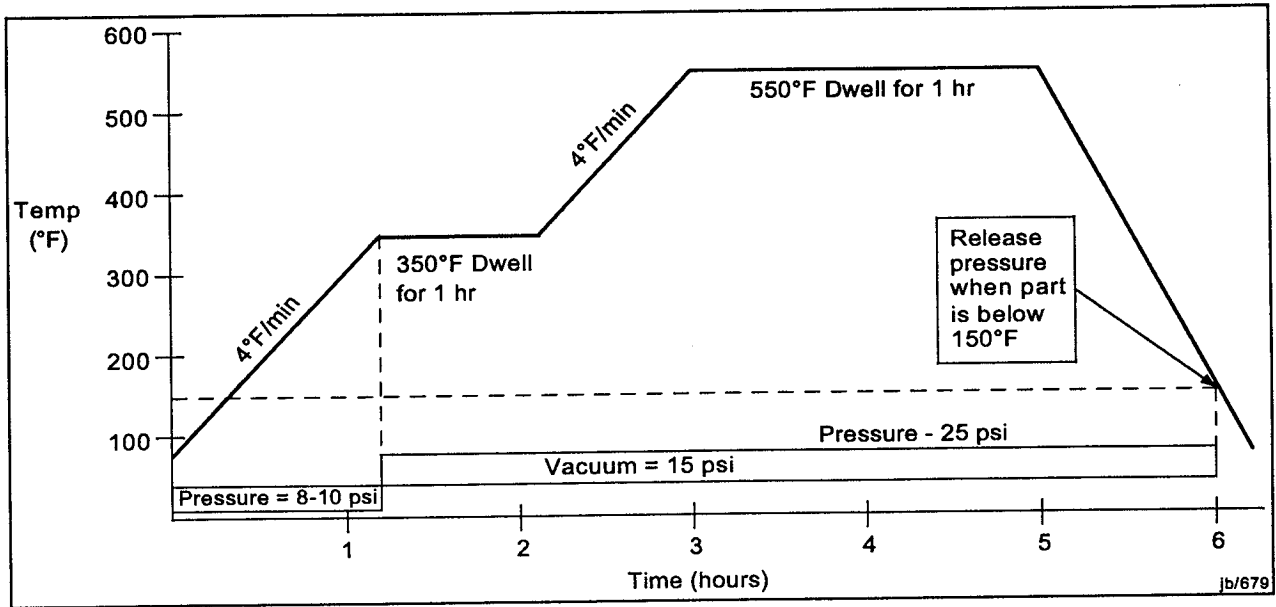


Figure 7.0-4. Autoclave Cure Cycle for FM 57

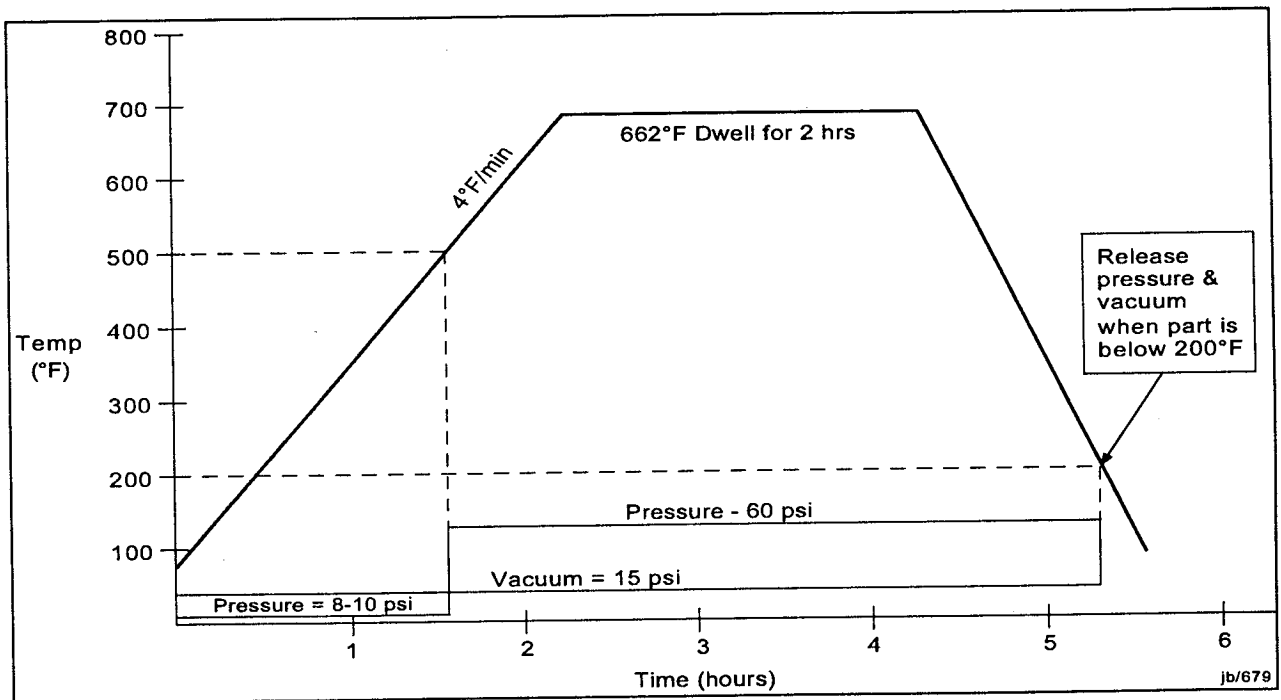


Figure 7.0-5. Autoclave Cure Cycle for K3A

Total thicknesses of the specimens, measured across the depth of the bonded coupons, were obtained in an attempt to assess the general thickness of the bondline. These data are provided in appendix C. They, however, did not appear to provide a reliable indication of bond thickness. They vary by more than the full thickness of the adhesive. A few of the specimens were then photomicrographed to measure actual thicknesses. These varied between 3 and 8 mils.

Although adherend measurements (thickness at multiple locations) were recorded before bonding, the adherend identifications were not visible after bonding. Therefore, bondline thickness could only be determined at the edges of the specimens with the aid of a microscope. The photomicrographs revealed significant variation in bondline thickness from one side of the specimen to the other, as well along one side of the specimen.

To quantify the quality of the bond, five specimens of each adhesive were ultimate-strength tested at RT. These data are shown in appendix D with a test date of 11/03/94. The bonded surface area was 1 in<sup>2</sup>, hence failure load and stress were identical. The FM 57 tests averaged 3,402 psi with the highest and lowest values equaling 3,850 and 3,050 psi, respectively. This test scatter equated to approximately  $\pm 12\%$ , a somewhat high value but within reason, particularly considering that the lowest value was above the 3,000 psi anticipated.

The K3A tests had an average strength of 2,670 psi. The highest and lowest values were 2,985 and 2,090 psi, respectively. This equates to a scatter ranging above and below the average from -21.7% to +11.8%, respectively. The spread is unusually high and the values were considerably lower (between 25% and 50%) than the 4,000 psi expected. Such low values would severely affect the planned tests because the fixtures were sized for bonds having a minimum shear strength of 3,000 psi. If uncorrected, the fixtures would have to be modified to accommodate the low strengths. The wide scatter and low values suggested that a problem existed with the bonding process and needed to be corrected. Close examination of the failed K3A specimens showed that the adhesive had unusually high porosity, preventing the surface area from being completely bonded. Several attempts to improve the bond failed. It was clear that additional development in surface preparations and cure cycles was necessary to remedy this impediment. This task was not funded to develop bonding techniques, so a search for another adhesive was initiated to replace K3A.

A separate problem occurred with the IM7/K3B laminated adherends. Several attempts to secondarily bond IM7/K3B laminates using K3A adhesive failed. One attempt to cocure the PMC adherends with K3A also proved unsuccessful. This highlighted a situation unique to high-temperature adhesives and laminated composites.

All known high-service-temperature adhesives require high-temperature processing. One of the best PMC candidates for high-temperature applications was K3B, a thermoplastic. This system had a glass transition temperature below 480°F. The peak bonding temperature for most high-temperature adhesives was 550°F. This caused the PMC to melt during the secondary bonding process. Even attempts to restrain the precured adherends were unsuccessful.

Initially, a 12- by 12-in trial laminate was fabricated and a through-transmission-ultrasonic (TTU) inspection was performed. Because of the thickness of the PMC adherends (100 plies), some difficulty was anticipated during the consolidation process. However, nondestructive inspection

(NDI) showed the laminate to be a very high quality consolidation (fig. 7.0-6). The thickness of the laminate was also uniform, with a maximum variation of 10 mils (fig. 7.0-7).

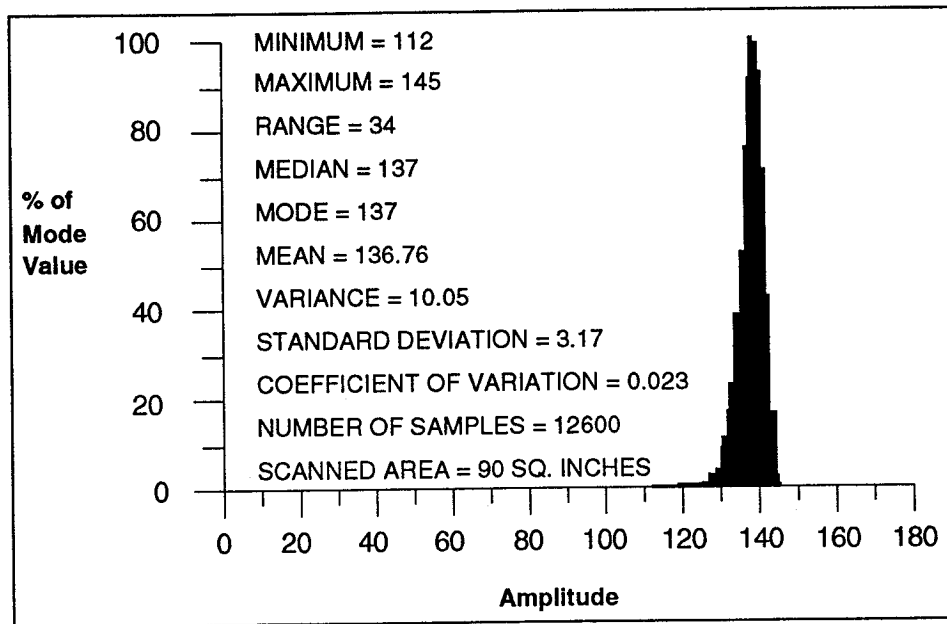


Figure 7.0-6. TTU Scan of 12- by 12-in, 100-ply, IM7/K3B Laminate

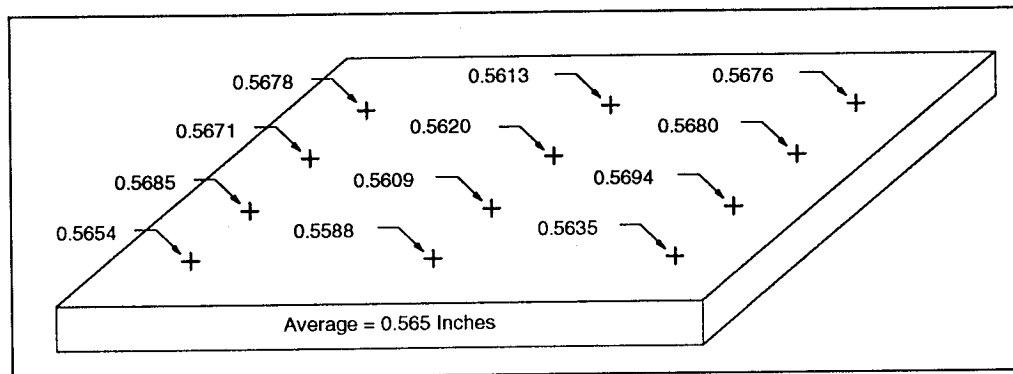


Figure 7.0-7. Measured Thicknesses on 12- by 12-in, 100-ply, IM7/K3B Laminate

This panel was then sectioned into ten 1- by 6-in coupons. A notch was cut from one end of each coupon to form the bonding surface of the thick-adherend type specimen. The notch was intended to be cut precisely to the centerline of the specimen, which contained a 0-deg ply for load transfer at the bondline. The milling of the notch was used as a feasibility study to machine the laminate to the exact depth. Ordinary methods of cutting to a predetermined depth proved to be inaccurate because the cutting depth varied with each coupon. Identifying the center ply in the shop during the milling operation required a microscope, not a standard piece of shop equipment. Applying a peel ply across the midsection of the notched region during the layup process to act as a visual marker was considered but not implemented. It could act as a barrier to the passage of volatiles during the consolidation process and result in a poor quality laminate. As a result of the milling difficulty, none of the notched coupons met specifications. These adherends, plus others fabricated later, were used in the bonding trials discussed in the following paragraphs.

Additional problems occurred when the applied pressure during bonding was less than the consolidation pressure. All K3B laminates were consolidated at 185 psi, but early bonding attempts were made at lower pressures. Some volatiles from the initial consolidation process remained within the laminate and expanded when the laminate temperature was again raised above or, possibly, even close to the melt temperature. Volatiles could have been released before reaching the melt temperature because the full 185-psi pressure was not applied. Prebonding thickness for each of the specimens was uniform at approximately 0.55 in. The thickness of each of the bonded specimens following cooling varied randomly between 0.55 and 0.75 in, due to swelling from residual volatiles. Considerable shifting of the plies was also observed. Shifted plies and pockets of swelling were evident throughout the bonded laminate. Figure 7.0-8 graphically exaggerates these conditions. Four of the coupons were ultimately strength-tested to obtain some indication of their strengths. They all failed between 1,875 and 2,120 lb. The bonded surface area was approximately 1 in<sup>2</sup>. Fully viable specimens were expected to sustain over 3,000 lb ultimate load.

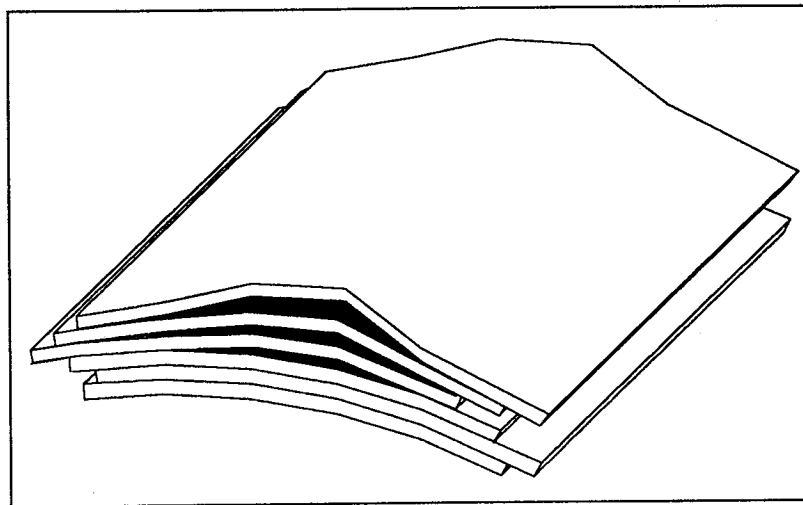


Figure 7.0-8. Condition of Laminate After Normal Bonding Process

The distortions and displacements within the lamina could possibly be avoided by using the full consolidation pressure during bonding, but this lessens the advantage of bonding components. Lower temperature curing thermosets may be able to avoid most of the problems encountered when reheating the laminate above the glass transition temperature, but the lower bonding temperatures may adversely affect the adhesive system's mechanical and durability properties. No high-temperature thermoset was identified that could potentially meet HSCT requirements and serve as a useful material alternative. Even with a lower temperature curing adhesive, some swelling, as seen in the K3B laminates, may occur if full pressure is not applied.

Difficulty achieving a uniform and desired K3A bondline thickness, first noted with the titanium adherends, was even more difficult with the composite adherends. This is believed to be partially due to the fact that this adhesive system did not have a scrim to maintain some separation between adherends. The fact that the PMC bonding surface did not remain rigid is believed to have aggravated the problem. Shims placed under the adherends to establish the adhesive thickness during the bonding process were not effective because the adherend did not retain its stiffness and the pressure caused adhesive flow. The softening of the adherends during the heat cycle made it

impossible to maintain the desired gap. Scrims in the adhesive could possibly overcome this problem, but no data were available to confirm this.

A second laminate was built with the center section containing a prefabricated notch along its length. The intent was to cut the laminate in half along the notched section, providing two wide coupons with ready-made notches. This would avoid the machining problem noted earlier. During the layup process, the notched section was replaced with a steel bar to provide support and pressure to the plies while being consolidated (fig. 7.0-9). After consolidation, examination of the laminate revealed distortions and voids near and around the notch. It was believed that this was a result of the plies not being carefully placed into position during the layup process. The laminate was nevertheless sectioned along its centerline, as originally planned, and was bonded together at 550°F, using 50-psi pressure. In essence, the bonded laminate turned out the same as the original specimens. The 50-psi pressure was not adequate to prevent laminate swelling. The laminate was again reconsolidated, using 185-psi pressure and 680°F temperature to see if the swelling could be expunged. The swelling was relieved, but ply slippage and distortions remained a problem. This bonded laminate was not used further.

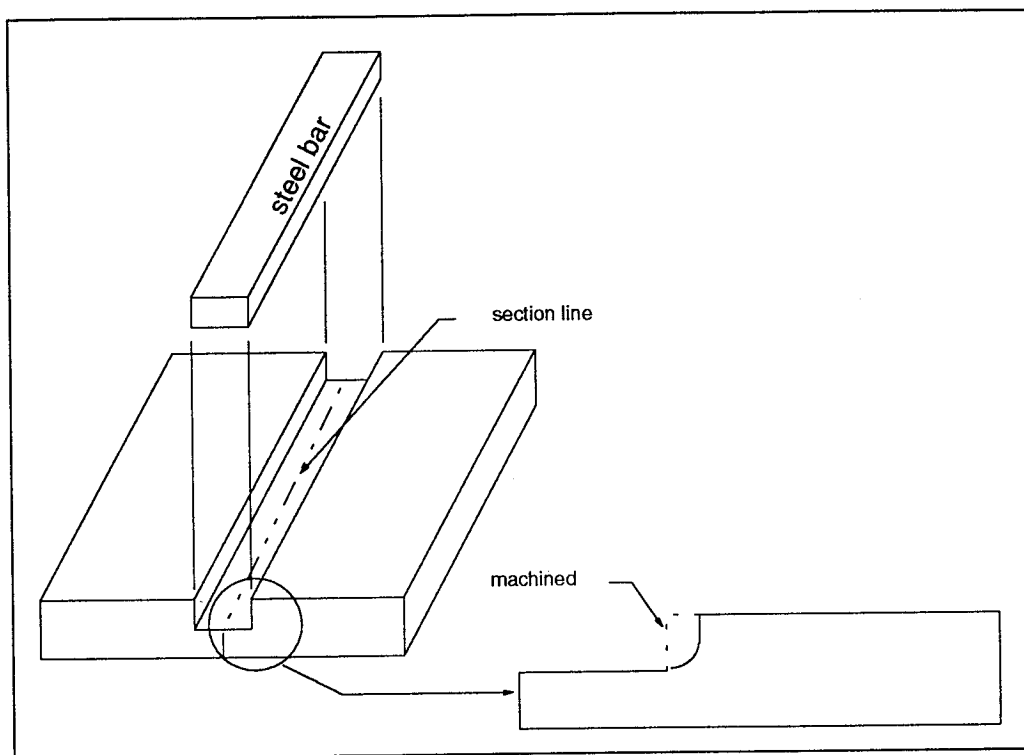


Figure 7.0-9. Prefabricated Notch in Laminate Using Metal Insert

It was felt at this point that the only feasible method to produce a satisfactory specimen for testing would require bonding the coupons at the same time the laminate was being consolidated. Achieving a proper bondline thickness was, however, still an issue. A third laminate was laid up as a one-piece thick-adherend laminate with notches more carefully fitted (fig. 7.0-10). Steel bars were inserted into the notches to provide support during the consolidation of the laminate. Two layers of adhesive (10 mils total thickness), to account for flow, were added along the center section, where the bond was intended. The preformed thick-adherend laminate was processed through a normal consolidation at 185-psi pressure and 680°F temperature.

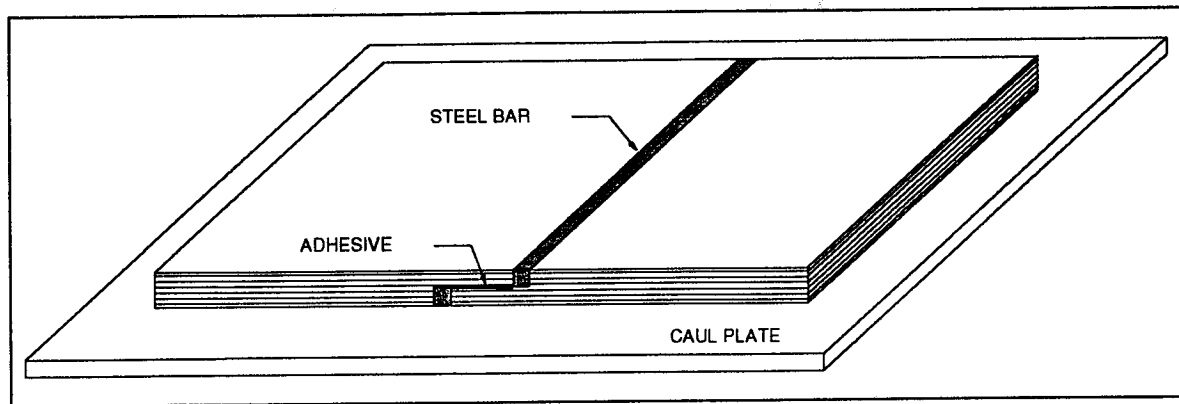


Figure 7.0-10. *Preformed Thick-Adherend Laminate Before Consolidation*

This process failed to produce a high-quality laminate because of four main reasons:

- a. The plies that butted up against the steel bars did not remain in place, causing nonuniform thicknesses and distortions along the edge of the notched section.
- b. The steel bars did not precisely match the thickness of the notch, due mostly to the variability of individual ply thicknesses, causing plies to drape over the bars instead of aligning flush with them. This caused the plies to develop a contour around the notched section instead of remaining flat.
- c. One of the two steel bars (upper) installed in the two notches was not rigidly supported by the caul plate as the other was and thus twisted during consolidation. This further added to the distortions previously observed in the other trials.
- d. Micrographs of the bondline showed it to be nonuniform and typically 1 mil in thickness. The intended thickness was 5 mils.

A fourth, 24-ply solid laminate was built containing the K3A adhesive, mounted on a scrim and placed at the middepth along the center section of the laminate. K3A adhesive normally does not have a scrim to help maintain the bondline thickness. This trial was used to determine whether a proper bondline could be achieved using a scrim, if a normal consolidation process were used for the bonding procedure. Although the consolidation of the laminate was successful, examination of the bondline disclosed no significant presence of adhesive. The adhesive apparently blended into the laminate resin. In light of these results, no further efforts were pursued to produce viable composite specimens. Continuation of a program to bond PMC adherends, using high-temperature adhesives and subjecting these specimens to long-term durability testing, would prove ineffectual. It was decided that the test program would not include composite adherends at this time.

None of the above problems were encountered with titanium adherends. However, a performance issue with FM 57 adhesive placed some doubts on its operational merits. Four specimens of FM 57 adhesive, bonded to titanium adherends, were used as part of a bond integrity and assessment study. These specimens were subjected to various fluids, transported, and handled while TTUs

were performed to evaluate the quality of their bond. On the basis of those measurements, each specimen was ranked by anticipated strength performance. To validate this rank, each specimen was ultimate-strength tested. Their strengths are given in appendix C with a test date of 12/13/94. The average of these strengths was 2,234 psi. This was 65% ( $2,234/3,402$ ) of the average strengths obtained earlier. Three of the four FM 57 specimens that were tested failed, on average 25% below the previous average. The fourth specimen failed more than 65% below the earlier average.

All specimens had been bonded at the same time and under identical conditions. It was unknown whether the ultrasonic tests performed on these four specimens or the additional handling to which they were exposed were responsible for the significantly lower strengths. It was thus decided that five additional FM 57 specimens would be ultimate-strength tested. These, also shown in appendix C with test date 1/13/95, gave an average strength of 3,183 psi. This was considerably higher than the previous test average (2,234 psi) but lower than the original (3,402 psi). However, if the highest test value (3,850 psi) of the original test series was ignored, the average strength differences between the 11/03/94 tests and the 1/13/95 tests were within approximately 100 psi (3,290 psi versus 3,183 psi). This appeared to demonstrate that little or no aging degradation had occurred over the 3-month time difference between bonding and strength testing. Therefore, it was concluded that the ultrasonic inspections or the handling of these specimens somehow damaged the specimens. The FM 57 adhesive, therefore, remained as a material choice for durability testing.

Because of previously noted problems using K3A adhesive (high void content and low strengths), other adhesives were considered to replace K3A for durability testing. The most promising candidates were R1-16 (modified K3A) and PETI-5. However, neither of these adhesives were believed to be sufficiently mature to enter into a durability program. Within a year, it was expected that these and perhaps other adhesives would have had time to demonstrate sufficient property traits to justify a moderate thermal-mechanical fatigue test evaluation. Until then, it was decided that only the FM 57 specimens would be evaluated using titanium adherends. This had the unfortunate consequence of changing the thrust of this program from a lapshear evaluation of model materials to a more exploratory phase, a reflection on the state of the art of high-temperature adhesive technology. Nevertheless, this approach avoided costly testing for inconsequential results.

Elimination of composite adherends and a hold on titanium specimens bonded with K3A adhesive reduced the number of planned tests significantly. As a result, several thermal and hydraulic fixtures, previously fabricated for these tests, became available, along with their designated slots in the thermal chamber. However, the thermal fixtures could not be indiscriminately used. They were sized to produce a specific strain at the planned peak temperature (300°F). A plan to accelerate flatwise tension testing was considered a suitable alternative for employing the fixtures and chamber slots. A preliminary flatwise tension specimen design was developed to verify the feasibility of using the thermal fixtures without modification (fig. 7.0-11). The thin adapters, pinned to the bonded specimens, were sized to produce designated loads across the bondline for the strains generated at peak temperatures. Timing and budget considerations were not fully examined before this report was completed. If included, the flatwise tension specimens would likely require an additional 3 to 6 months before they could be available for testing.

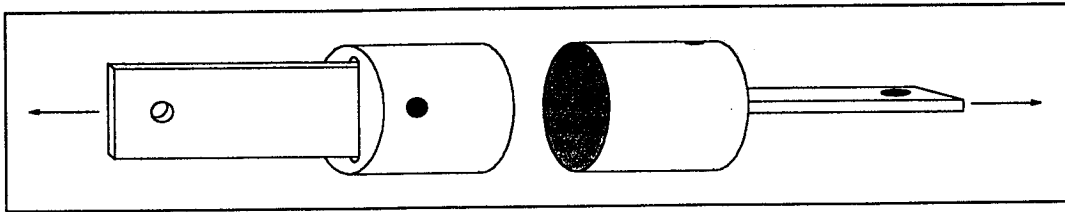


*Figure 7.0-11. Proposed Flatwise Tension Specimen for Thermal Fixture Testing*

No durability testing had begun before the completion of this phase of NASA funding. This task was, however, carried forward to the High-Speed Research (HSR) II, NASA-funded contract NAS1-20220, Task Assignment No. 15, "Materials Durability." Durability testing and reporting will be performed under that project.

## 8.0 CONCLUSIONS

The efforts completed under this project included research, planning, and fabrication of adhesively bonded specimens for long-term durability testing. The conclusions derived are restricted to efforts expended up to the initiation of thermal cyclic testing.

- a. Characterization of adhesives exposed to the combination of thermal and mechanical cycling over long durations has not been significantly studied. This is critically true for high-temperature adhesives prescribed for primary structural applications.
- b. Basic characterization of high-temperature adhesives is necessary before they can be incorporated into primary structure. This can efficiently be achieved for thermal-mechanical behavior through separate studies of shear and tension strength degradation on bonded joints. Understanding the individual behavior of shear and tension degradation will facilitate their integration into a combined loading prediction model.
- c. Bonded thick-adherend specimens are relatively simple and inexpensive to fabricate and test, while providing a nearly pure shear load distribution. Bonded flatwise tension specimens, mounted on self-aligning gimbals, provide an economical method to investigate peel or pulloff load capability.
- d. Low-cost thermal-mechanical testing can be achieved through fixtures designed to induce loads using the principle of differential coefficients of thermal expansion. This requires the restraining part of the fixture to be relatively fixed, regardless of temperature, and the load initiator to expand markedly with temperature.
- e. Secondary bonding of laminated composites with high-temperature adhesives is not practical if the curing temperature of the adhesive is above the glass transition temperature of the laminate. Bonding above this temperature has profound effects on the laminate through postcuring, softening, and residual volatile gassing of the laminate. This causes severe distortions and deterioration.
- f. Most available high-temperature adhesives cure above the glass transition temperature of today's candidate HSCT composites.
- g. FM57 adhesive was successfully used to bond Ti adherends for the fabrication of thick adherend test specimens.
- h. K3A adhesive was not successfully used to bond Ti adherends for the fabrication of thick adherend test specimens. Porosity in the bond line appeared to be the cause of low strength values. Cure process optimization may resolve this problem.
- i. K3A adhesive was not successfully used to bond composite (IM7/K3B) adherends for the fabrication of thick adherend test specimens. Delamination of the composite adherend occurred due to heating the material above  $T_g$  during the bonding process. Cocuring the adhesive and prepreg may be the only feasible method of bonding K3A to K3B. No attempt was made to bond K3B with FM57 as similar results were expected.

## 9.0 RECOMMENDATIONS

- a. Additional effort is required to develop PMC and adhesive materials or processes that enable these material combinations to be secondarily bonded. Difficulties experienced with fabricating specimens for this program suggest that the need is acute.
- b. Task 15 of NASA contract NAS1-20220 should subject titanium lapshear specimens bonded with FM 57 adhesive to durability testing.
- c. Task 15 of NASA contract NAS1-20220 should explore flatwise tension specimens using the materials listed in item b.
- d. Additional attempts should be made to bond lapshear specimens with K3A adhesive.

## 10.0 BIBLIOGRAPHY

1. Loop, R. K., "Resistance of Metalbond Structure to Aircraft Inservice Environment," Final Report D6-49771TN, Boeing Commercial Airplane Company, July 1982.
2. Krieger Jr., R. B., "Stress Analysis of Metal-to-Metal Bonds in Hostile Environment," 22nd National SAMPE Symposium, San Diego, California, April 1977.
3. Marceau, J. A., "Cyclic Stress Testing of Adhesive Bonds," 22nd National SAMPE Symposium, San Diego, California, April 1977, Boeing Document D6-44386.
4. Potter, D. L., "Primary Adhesively Bonded Structure Technology (PABST), Design Handbook for Adhesive Bonding," Final Report AFFDL-TR-79-3129, November 1979.
5. McLellan, D., Personal Notes
6. Johnson, W. S., "A Fracture Mechanics Approach for Designing Adhesively Bonded Joints," *Delamination and Debonding of Materials*, ASTM STP 876, W. S. Johnson, editor, American Society for Testing and Materials, Philadelphia, 1985, pp. 189-199.
7. Hart-Smith, L. J., "Adhesive-Bonded Joints for Composites - Phenomenological Considerations," Technology Conferences Association, Conference on Adhesive Composites Technology, El Segundo, California, March 1978.
8. Hart-Smith, L. J., "Adhesive-Bonded Double-Lap Joints," NASA CR-112235, 1973.

## APPENDIX A - COUPON ANALYSIS RESULTS

Summary conclusions of the analytical efforts targeted at providing a specimen with a uniform shear stress along the length of the bondline were provided in section 4.1. This appendix presents additional details. All analysis assumed elastic behavior; an elastic-plastic analysis would have provided greater accuracy but was beyond the scope of the program. Also, it should be noted that conclusions regarding joint shapes have been experimentally verified elsewhere.

Study variables included adhesive and adherend moduli, as well as joint profile shape. Some of the pertinent results are shown in figures A-1 and A-2.

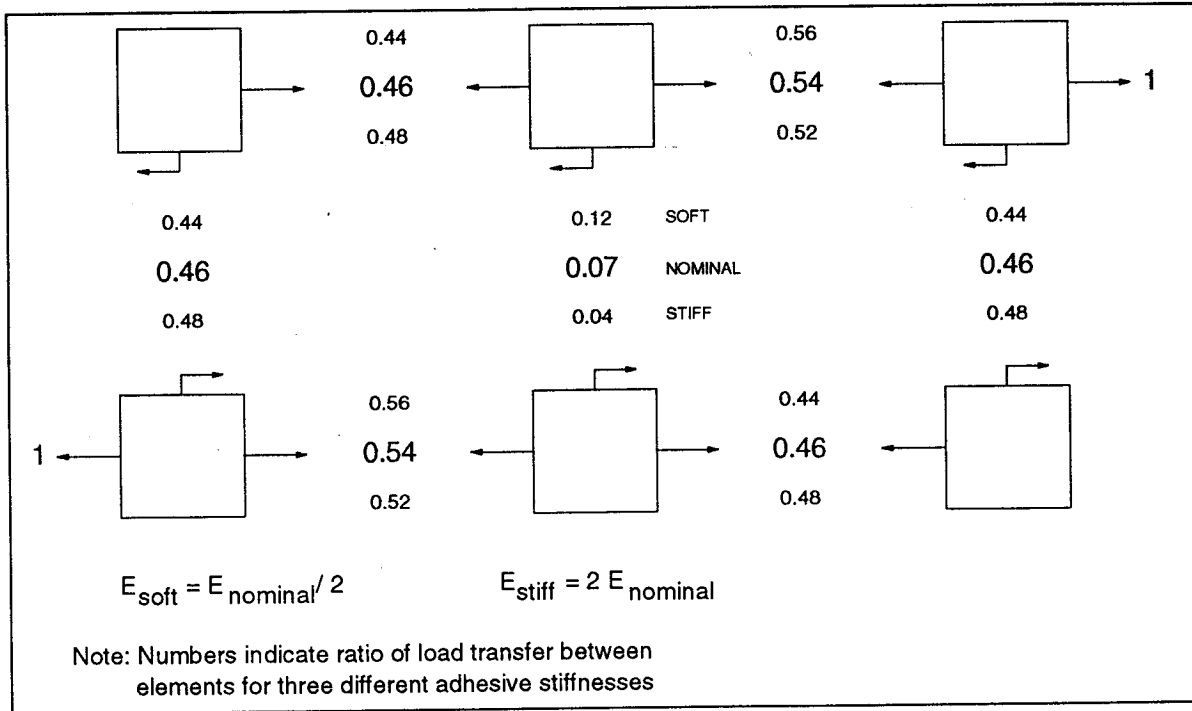


Figure A-1. Variation of Load Transfer Through a Bonded Joint Using Soft, Nominal, and Stiff Modulus Adhesives

The main purpose of the analyses was to identify techniques that would more uniformly distribute the loads across the bondline. From figure A-1, adhesive stiffnesses clearly have some influence on load transfers across bondlines, everything else remaining equal. However, it is also clear that the variation is minor. Softer adhesives better distribute the loads but high peak loads remain at the ends of the bond and near zero loads remain at the center section, regardless of the adhesive. Therefore, it was concluded that adhesive stiffness was not important enough to influence the adhesive selection.

The effect of bonding two adherends together, each with a different moduli, such as steel with titanium or two laminates with dissimilar longitudinal moduli, or even two identical materials and layups but with different thicknesses, can significantly cause an adjustment in the distribution of load transfer across the bondline (fig. A-2). However, the principal adjustments occur at the ends of the lap joints and very little between them, particularly at the center. Just as was seen with adhesive stiffness variations, no appreciable uniform load spreading was observed, and hence,

stiffness mismatching of the adherends was not determined to be beneficial in producing uniform loads across the joint.

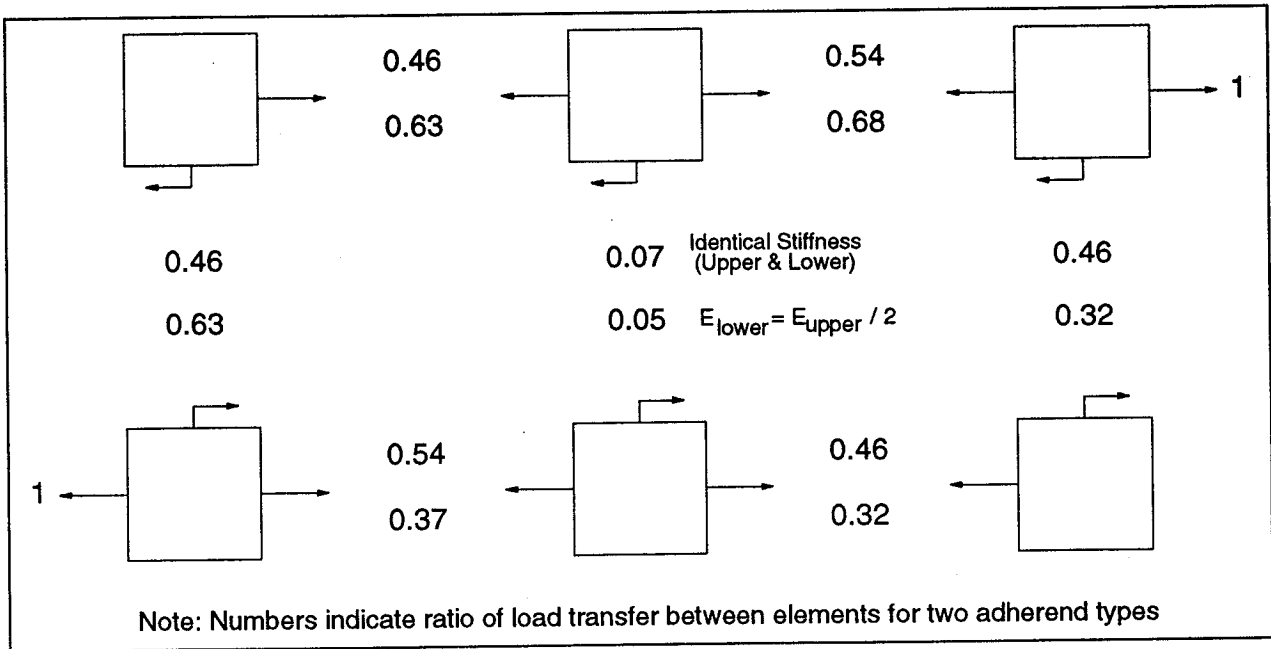


Figure A-2. Variation of Load Transfer Through a Bonded Joint With Identical and Dissimilar Adherend Stiffnesses

Tapered adherends have long been known to improve the performance of adhesive bond strengths. The gradually thickening adherend initially has very low stiffness at the end of the taper and, hence, is unable to support very much shear load transfer. As the thickness increases, the stiffness proportionally increases and thus greater load transfer is possible. If the opposing adherend narrows, it progressively loses its capability to carry load and, consequently, transfers its load faster than a nontapering adherend. These effects are summarized in figure A-3. As seen in nontapering joint (a), 70% of the load transfer occurs at the end elements of the joint and the remaining 30% is transferred between the end elements. Interestingly, more than 40% of the central area of the joint transfers only 10% of the load. Dual-tapering joint (b), however, clearly shows that the shear load transfer is perfectly uniform across the entire length of the joint. This type of joint appears to achieve the goal of uniform load distribution. However, it was not used in this task because of other potential problems discussed later.

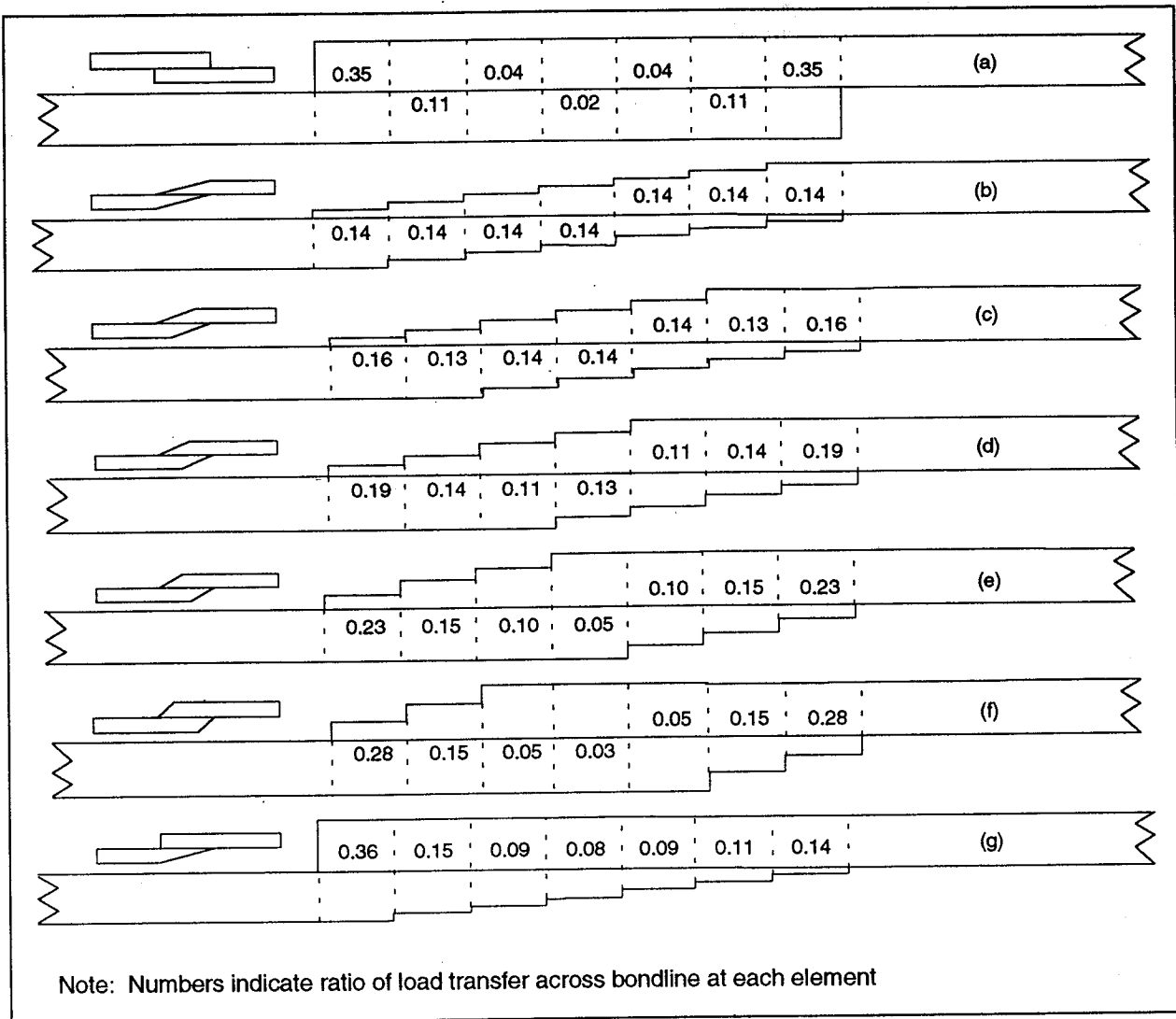


Figure A-3. Effects of Adherend Tapering on Shear Load Transfer Across Bondlines

It was of interest to understand how shifting of the tapered adherends, relative to each other, affected load transfer. These effects are shown in joints (c) through (f). As the tapering of the joints tend to become less and less aligned (i.e., the stiffnesses between the upper and lower adherends do not correspondingly change to provide a combined stiffness that is constant at any cross section), the end elements tend to progressively increase their share of the load. As long as both adherends maintain a taper, regardless of their relative position, their end-shear loads will be reduced when compared with nontapered joints. However, as compared between joints (a) and (f), the differences may not appear to be great, particularly when considering the potential benefit of joint (b). It should not be overlooked that joint (f) will theoretically offer a 25% ( $0.35/0.28$ ) stronger bond than joint (a). This, of course, ignores other factors that can influence results, of which peel stresses are certainly players.

Joint (g) is shown to demonstrate the effect of bonding a tapered adherend with a uniform-thickness adherend. The tapered end of the adherend transmits the same amount of shear load as bi-tapered joints, such as joint (b), but the other end of the bond point transfers nearly the same

shear load as joint (a). This type of joint, from only a shear-load transfer perspective, does not offer any advantages.

The overall conclusion from the above study was that most modifiable characteristics in joints could not be made to significantly contribute to a uniform shear-load transfer. The one exception was the equally tapering adherends. This configuration was therefore considered for the thick-adherend specimens. An example of its appearance is given in figure A-4.

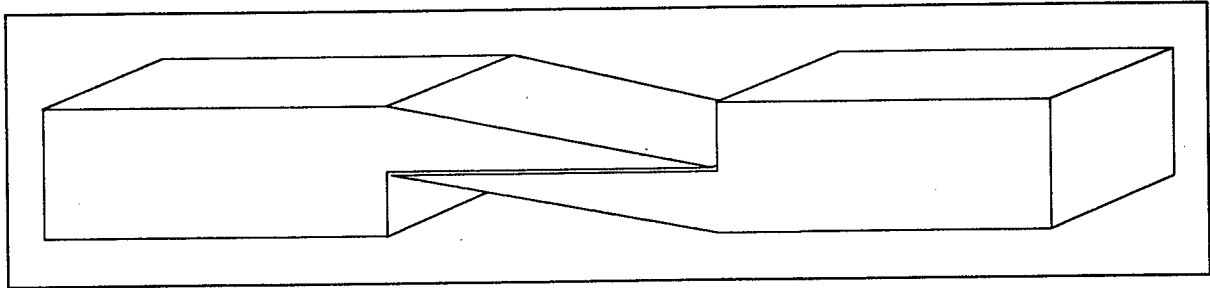


*Figure A-4. Thick-Adherend Specimen With Tapered Joints*

Although the thick-adherend tapered joint appears to meet all objectives for durability testing, it was discounted for some basic concerns. Half of the specimens were to be manufactured with titanium and the other half with composite materials. The principal concern was with the laminated composites. In order to taper the joint, surface plies would have to be progressively removed, preventing the laminate from remaining symmetrical about any cross-sectional cut. This can have a significant effect on both the finished shape of the part and on internal load distributions. After trimming the part to specifications, internal residual thermal stresses can cause the part to warp. Bonding would then become a problem and disbonding stresses would likely be a consequence. External loads applied to an unsymmetrical laminate also cause twisting and bending. The source of these combined distortions could conceivably create undesirable loads that would prevent achieving the uniformity that was initially intended. Long-term durability exposure could have additional detrimental effects on results. Without considerable experimentation, including long-exposure periods, tapered thick-adherend specimens were not considered ideal.

## APPENDIX B - TITANIUM COUPON MEASUREMENTS

Figure B-1 gives measurements obtained from 25 randomly selected titanium coupons.

| Measured Thicknesses, Inches |       |       |       |       |       |       |       |       |
|------------------------------|-------|-------|-------|-------|-------|-------|-------|-------|
| Identifiers                  |       |       |       |       |       |       |       |       |
| Specimens                    | A     | B     | C     | D     | E     | F     | G     | H     |
| S-1                          | 0.548 | 0.548 | 0.276 | 0.995 | 0.995 | 0.995 | 0.502 | 0.376 |
| S-2                          | 0.548 | 0.548 | 0.274 | 0.996 | 0.995 | 0.995 | 0.500 | 0.383 |
| S-3                          | 0.545 | 0.545 | 0.271 | 0.994 | 0.995 | 0.997 | 0.500 | 0.382 |
| S-4                          | 0.550 | 0.550 | 0.275 | 0.994 | 0.994 | 0.994 | 0.500 | 0.381 |
| S-5                          | 0.555 | 0.551 | 0.274 | 0.993 | 0.993 | 0.993 | 0.501 | 0.375 |
| S-6                          | 0.551 | 0.550 | 0.274 | 0.995 | 0.994 | 0.995 | 0.501 | 0.374 |
| S-7                          | 0.550 | 0.551 | 0.272 | 0.994 | 0.994 | 0.993 | 0.501 | 0.374 |
| S-8                          | 0.548 | 0.550 | 0.273 | 0.994 | 0.994 | 0.994 | 0.500 | 0.372 |
| S-9                          | 0.550 | 0.551 | 0.272 | 0.995 | 0.995 | 0.995 | 0.502 | 0.373 |
| S-10                         | 0.546 | 0.550 | 0.271 | 0.996 | 0.995 | 0.996 | 0.501 | 0.376 |
| S-11                         | 0.550 | 0.552 | 0.277 | 0.996 | 0.997 | 0.995 | 0.501 | 0.386 |
| S-12                         | 0.548 | 0.547 | 0.277 | 0.998 | 0.997 | 1.000 | 0.497 | 0.376 |
| S-13                         | 0.552 | 0.552 | 0.276 | 0.992 | 0.993 | 0.993 | 0.500 | 0.378 |
| S-14                         | 0.551 | 0.551 | 0.275 | 0.995 | 0.995 | 0.995 | 0.500 | 0.376 |
| S-15                         | 0.554 | 0.555 | 0.279 | 0.995 | 0.994 | 0.995 | 0.500 | 0.378 |
| S-16                         | 0.555 | 0.554 | 0.273 | 0.997 | 0.996 | 0.995 | 0.500 | 0.372 |
| S-17                         | 0.548 | 0.547 | 0.274 | 1.000 | 1.000 | 0.999 | 0.502 | 0.378 |
| S-18                         | 0.549 | 0.550 | 0.272 | 1.000 | 0.996 | 0.994 | 0.500 | 0.376 |
| S-19                         | 0.543 | 0.543 | 0.274 | 0.998 | 0.992 | 0.993 | 0.500 | 0.379 |
| S-20                         | 0.550 | 0.549 | 0.274 | 0.995 | 0.996 | 0.995 | 0.501 | 0.375 |
| S-21                         | 0.549 | 0.548 | 0.276 | 0.996 | 0.993 | 0.992 | 0.501 | 0.378 |
| S-22                         | 0.553 | 0.552 | 0.277 | 0.998 | 0.992 | 0.997 | 0.502 | 0.372 |
| S-23                         | 0.551 | 0.554 | 0.274 | 0.994 | 0.995 | 0.995 | 0.500 | 0.376 |
| S-24                         | 0.549 | 0.546 | 0.277 | 0.995 | 0.997 | 0.998 | 0.500 | 0.372 |
| S-25                         | 0.549 | 0.548 | 0.272 | 0.996 | 0.997 | 0.999 | 0.502 | 0.379 |
| Average                      | 0.550 | 0.550 | 0.274 | 0.996 | 0.995 | 0.995 | 0.501 | 0.377 |
| Specification                | 0.550 | 0.550 | 0.275 | 1.000 | 1.000 | 1.000 | 0.502 | 0.375 |

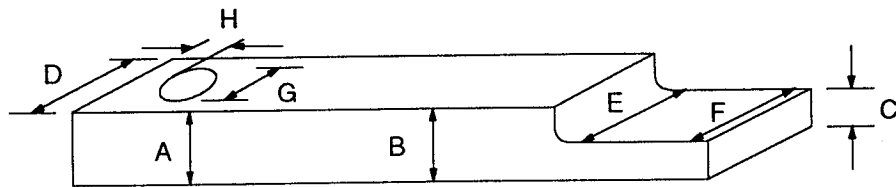


Figure B-1. Measurements From 25 Randomly Selected Titanium Coupons

## APPENDIX C - BONDED SPECIMEN MEASUREMENTS

Measurements from 50 titanium-bonded specimens were recorded. Half were bonded with K3A (fig. C-1) and the other half with FM 57 (fig. C-2) adhesive. These give a relative measure of bondline uniformity.

| Specimens     | Measured Thicknesses, Inches |       |       |       |       |         |       |
|---------------|------------------------------|-------|-------|-------|-------|---------|-------|
|               | Identifiers                  |       |       |       |       |         |       |
|               | A                            | B     | C     | D     | E     | Average | F     |
| K3A - 1       | 0.550                        | 0.547 | 0.548 | 0.549 | 0.546 | 0.548   | 0.988 |
| K3A - 2       | 0.550                        | 0.550 | 0.551 | 0.551 | 0.551 | 0.551   | 0.997 |
| K3A - 3       | 0.547                        | 0.546 | 0.556 | 0.546 | 0.545 | 0.546   | 0.992 |
| K3A - 4       | 0.550                        | 0.549 | 0.550 | 0.551 | 0.550 | 0.550   | 0.969 |
| K3A - 5       | 0.548                        | 0.548 | 0.558 | 0.549 | 0.548 | 0.548   | 0.940 |
| K3A - 6       | 0.550                        | 0.551 | 0.552 | 0.553 | 0.553 | 0.552   | 0.957 |
| K3A - 7       | 0.553                        | 0.550 | 0.553 | 0.553 | 0.550 | 0.552   | 0.970 |
| K3A - 8       | 0.556                        | 0.556 | 0.556 | 0.556 | 0.555 | 0.556   | 0.977 |
| K3A - 9       | 0.553                        | 0.553 | 0.553 | 0.554 | 0.553 | 0.553   | 0.962 |
| K3A - 10      | 0.554                        | 0.552 | 0.553 | 0.554 | 0.552 | 0.553   | 0.973 |
| K3A - 11      | 0.550                        | 0.550 | 0.551 | 0.552 | 0.552 | 0.551   | 0.984 |
| K3A - 12      | 0.552                        | 0.551 | 0.552 | 0.552 | 0.551 | 0.552   | 0.983 |
| K3A - 13      | 0.552                        | 0.551 | 0.551 | 0.552 | 0.551 | 0.551   | 0.968 |
| K3A - 14      | 0.553                        | 0.550 | 0.551 | 0.553 | 0.551 | 0.552   | 0.963 |
| K3A - 15      | 0.548                        | 0.548 | 0.548 | 0.548 | 0.547 | 0.548   | 0.960 |
| K3A - 16      | 0.552                        | 0.552 | 0.552 | 0.551 | 0.551 | 0.552   | 0.966 |
| K3A - 17      | 0.550                        | 0.550 | 0.551 | 0.551 | 0.551 | 0.551   | 0.960 |
| K3A - 18      | 0.550                        | 0.550 | 0.550 | 0.549 | 0.550 | 0.550   | 0.978 |
| K3A - 19      | 0.549                        | 0.549 | 0.549 | 0.550 | 0.549 | 0.549   | 0.984 |
| K3A - 20      | 0.550                        | 0.550 | 0.550 | 0.550 | 0.551 | 0.550   | 0.961 |
| K3A - 21      | 0.549                        | 0.548 | 0.548 | 0.549 | 0.548 | 0.548   | 0.969 |
| K3A - 22      | 0.546                        | 0.544 | 0.546 | 0.546 | 0.544 | 0.545   | 0.966 |
| K3A - 23      | 0.548                        | 0.548 | 0.547 | 0.548 | 0.547 | 0.548   | 0.965 |
| K3A - 24      | 0.549                        | 0.548 | 0.549 | 0.548 | 0.548 | 0.548   | 0.970 |
| K3A - 25      | 0.549                        | 0.549 | 0.550 | 0.550 | 0.549 | 0.549   | 0.966 |
| Average       | 0.550                        | 0.550 | 0.550 | 0.551 | 0.550 | 0.550   | 0.971 |
| Specification | 0.555                        | 0.555 | 0.555 | 0.555 | 0.555 | 0.555   | 1.000 |

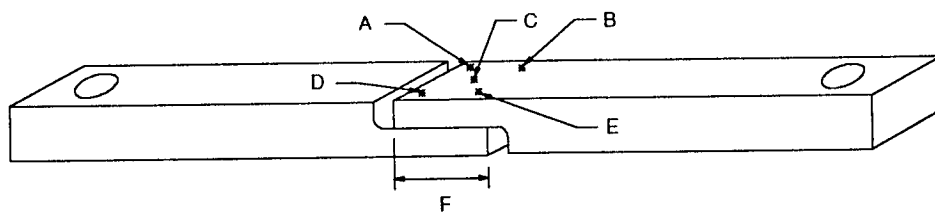


Figure C-1. Measurements of Specimens Bonded With K3A

| Specimens     | Measured Thicknesses, Inches |       |       |       |       |         |       |
|---------------|------------------------------|-------|-------|-------|-------|---------|-------|
|               | Identifiers                  |       |       |       |       |         |       |
|               | A                            | B     | C     | D     | E     | Average | F     |
| FM 57 - 1     | 0.554                        | 0.546 | 0.545 | 0.544 | 0.545 | 0.545   | *     |
| FM 57 - 2     | 0.549                        | 0.550 | 0.547 | 0.546 | 0.547 | 0.548   | *     |
| FM 57 - 3     | 0.550                        | 0.552 | 0.552 | 0.550 | 0.551 | 0.551   | *     |
| FM 57 - 4     | 0.552                        | 0.552 | 0.553 | 0.552 | 0.552 | 0.552   | *     |
| FM 57 - 5     | 0.550                        | 0.550 | 0.550 | 0.550 | 0.550 | 0.550   | *     |
| FM 57 - 6     | 0.552                        | 0.553 | 0.552 | 0.551 | 0.551 | 0.552   | 0.980 |
| FM 57 - 7     | 0.549                        | 0.551 | 0.549 | 0.547 | 0.550 | 0.549   | 0.983 |
| FM 57 - 8     | 0.552                        | 0.552 | 0.552 | 0.552 | 0.552 | 0.552   | 0.980 |
| FM 57 - 9     | 0.552                        | 0.552 | 0.552 | 0.552 | 0.552 | 0.552   | 0.984 |
| FM 57 - 10    | 0.552                        | 0.552 | 0.553 | 0.552 | 0.552 | 0.552   | 0.990 |
| FM 57 - 11    | 0.550                        | 0.551 | 0.552 | 0.551 | 0.551 | 0.551   | 0.959 |
| FM 57 - 12    | 0.551                        | 0.552 | 0.552 | 0.552 | 0.552 | 0.552   | 0.962 |
| FM 57 - 13    | 0.550                        | 0.552 | 0.552 | 0.549 | 0.552 | 0.551   | 0.958 |
| FM 57 - 14    | 0.547                        | 0.547 | 0.547 | 0.546 | 0.547 | 0.547   | 0.965 |
| FM 57 - 15    | 0.552                        | 0.552 | 0.552 | 0.552 | 0.553 | 0.552   | 0.960 |
| FM 57 - 16    | 0.553                        | 0.553 | 0.553 | 0.553 | 0.553 | 0.553   | 0.959 |
| FM 57 - 17    | 0.550                        | 0.551 | 0.550 | 0.549 | 0.550 | 0.550   | 0.977 |
| FM 57 - 18    | 0.553                        | 0.551 | 0.553 | 0.544 | 0.543 | 0.549   | 0.979 |
| FM 57 - 19    | 0.547                        | 0.546 | 0.545 | 0.546 | 0.544 | 0.546   | 0.985 |
| FM 57 - 20    | 0.551                        | 0.552 | 0.551 | 0.550 | 0.551 | 0.551   | 0.989 |
| FM 57 - 21    | 0.552                        | 0.552 | 0.552 | 0.552 | 0.552 | 0.552   | 0.956 |
| FM 57 - 22    | 0.550                        | 0.550 | 0.550 | 0.550 | 0.550 | 0.550   | 0.983 |
| FM 57 - 23    | 0.549                        | 0.549 | 0.549 | 0.549 | 0.549 | 0.549   | 0.952 |
| FM 57 - 24    | 0.551                        | 0.551 | 0.550 | 0.549 | 0.550 | 0.550   | 0.985 |
| FM 57 - 25    | 0.553                        | 0.553 | 0.553 | 0.554 | 0.543 | 0.553   | 0.959 |
| Average       | 0.551                        | 0.551 | 0.551 | 0.550 | 0.550 | 0.550   | 0.972 |
| Specification | 0.555                        | 0.555 | 0.555 | 0.555 | 0.555 | 0.555   | 1.000 |

\* Data not available.

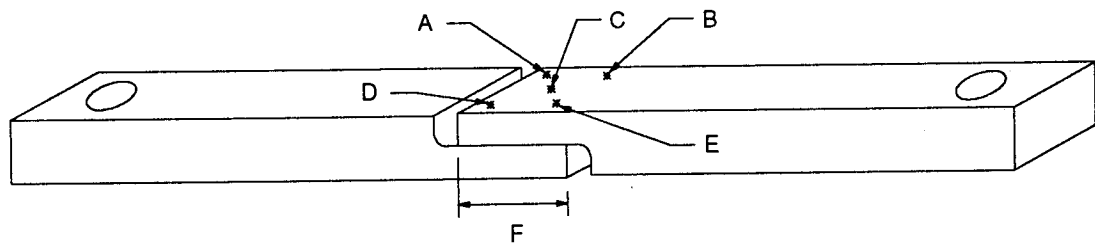


Figure C-2. Measurements of Specimens Bonded With FM 57

## APPENDIX D - ULTIMATE-STRENGTH DATA FOR THICK-ADHEREND SPECIMENS

The ultimate-strength data from thick-adherend test specimens are provided in figures D-1 and D-2. Figure D-1 contains data from K3A adhesive specimens, and figure D-2 contains data from FM 57 adhesive specimens. All specimens were unaged and tested at RT.

| Specimen Number            | Failure Stress (psi) | Failure Mode | Date Tested |
|----------------------------|----------------------|--------------|-------------|
| K3A-Ti-8                   | 2,860                | adhesive     | 11/03/94    |
| K3A-Ti-10                  | 2,090                | adhesive     | 11/03/94    |
| K3A-Ti-16                  | 2,440                | adhesive     | 11/03/94    |
| K3A-Ti-23                  | 2,985                | adhesive     | 11/03/94    |
| K3A-Ti-25                  | 2,975                | adhesive     | 11/03/94    |
| <b>Average (11/03/94)</b>  | <b>2,670</b>         | adhesive     |             |
| K3A-Ti-6                   | 2,975                | adhesive     | 12/13/94    |
| K3A-Ti-7                   | 2,575                | adhesive     | 12/13/94    |
| K3A-Ti-9                   | 2,750                | adhesive     | 12/13/94    |
| K3A-Ti-11                  | 2,600                | adhesive     | 12/13/94    |
| K3A-Ti-12                  | 2,675                | adhesive     | 12/13/94    |
| K3A-Ti-13                  | 2,940                | adhesive     | 12/13/94    |
| K3A-Ti-14                  | 1,840                | adhesive     | 12/13/94    |
| K3A-Ti-15                  | 3,300                | adhesive     | 12/13/94    |
| K3A-Ti-17                  | 3,050                | adhesive     | 12/13/94    |
| K3A-Ti-18                  | 2,775                | adhesive     | 12/13/94    |
| K3A-Ti-19                  | 2,800                | adhesive     | 12/13/94    |
| K3A-Ti-20                  | 2,650                | adhesive     | 12/13/94    |
| K3A-Ti-21                  | 2,685                | adhesive     | 12/13/94    |
| K3A-Ti-22                  | 2,875                | adhesive     | 12/13/94    |
| K3A-Ti-24                  | 3,000                | adhesive     | 12/13/94    |
| <b>Average (12/13/94)</b>  | <b>2,766</b>         | adhesive     |             |
| K3A-Ti-1                   | 2,875                | adhesive     | 1/17/95     |
| K3A-Ti-2                   | 2,925                | adhesive     | 1/17/95     |
| K3A-Ti-3                   | 3,100                | adhesive     | 1/17/95     |
| K3A-Ti-4                   | 2,865                | adhesive     | 1/17/95     |
| K3A-Ti-5                   | 2,920                | adhesive     | 1/17/95     |
| <b>Average (1/17/95)</b>   | <b>2,937</b>         | adhesive     |             |
| <b>K3A Overall Average</b> | <b>2,781</b>         | adhesive     |             |

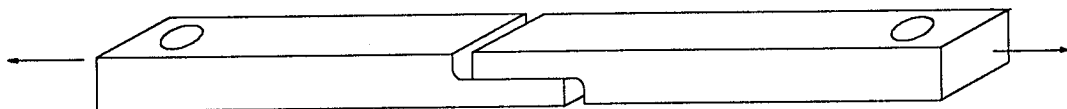


Figure D-1. Ultimate-Strength Data From Thick-Adherend Specimens With K3A Adhesive

| Specimen Number              | Failure Stress (psi) | Failure Mode | Date Tested |
|------------------------------|----------------------|--------------|-------------|
| FM 57-Ti-7                   | 3,850                | cohesive     | 11/03/94    |
| FM 57-Ti-8                   | 3,275                | cohesive     | 11/03/94    |
| FM 57-Ti-9                   | 3,395                | cohesive     | 11/03/94    |
| FM 57-Ti-10                  | 3,050                | cohesive     | 11/03/94    |
| FM 57-Ti-11                  | 3,440                | cohesive     | 11/03/94    |
| <b>Average (11/03/94)</b>    | <b>3,402</b>         | cohesive     |             |
| * FM 57-Ti-1                 | 2,745                | cohesive     | 12/13/94    |
| * FM 57-Ti-2                 | 2,490                | cohesive     | 12/13/94    |
| * FM 57-Ti-4                 | 1,100                | cohesive     | 12/13/94    |
| * FM 57-Ti-5                 | 2,600                | cohesive     | 12/13/94    |
| <b>Average (12/13/94)</b>    | <b>2,234</b>         | cohesive     |             |
| FM 57-Ti-14                  | 2,790                | cohesive     | 1/13/95     |
| FM 57-Ti-16                  | 3,300                | cohesive     | 1/13/95     |
| FM 57-Ti-18                  | 3,100                | cohesive     | 1/13/95     |
| FM 57-Ti-20                  | 3,325                | cohesive     | 1/13/95     |
| FM 57-Ti-24                  | 3,400                | cohesive     | 1/13/95     |
| <b>Average (1/13/95)</b>     | <b>3,183</b>         | cohesive     |             |
| <b>FM 57 Overall Average</b> | <b>2,990</b>         | cohesive     |             |

\* Specimens subjected to ultrasonic inspections and substances to enhance transmissions.

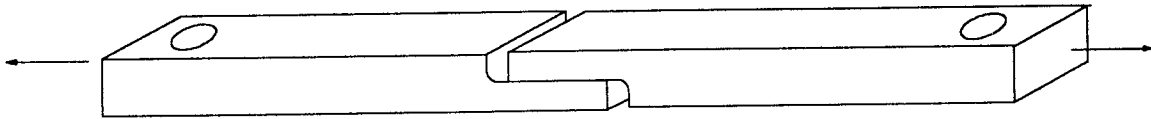


Figure D-2. Ultimate-Strength Data From Thick-Adherend Specimens With FM 57 Adhesive

# REPORT DOCUMENTATION PAGE

*Form Approved*  
OMB No. 0704-0188

Public reporting burden for this collection of information is estimated to average 1 hour per response, including the time for reviewing instructions, searching existing data sources, gathering and maintaining the data needed, and completing and reviewing the collection of information. Send comments regarding this burden estimate or any other aspect of this collection of information, including suggestions for reducing this burden, to Washington Headquarters Services, Directorate for Information Operations and Reports, 1215 Jefferson Davis Highway, Suite 1204, Arlington, VA 22202-4302, and to the Office of Management and Budget, Paperwork Reduction Project (0704-0188), Washington, DC 20503.

|  |   |  |   |  |
|--|---|--|---|--|
| <b>1. AGENCY USE ONLY (Leave blank)</b>  |   | <b>2. REPORT DATE</b><br>August 1995           | <b>3. REPORT TYPE AND DATES COVERED</b><br>Contractor Report              |  |
| <b>4. TITLE AND SUBTITLE</b><br>Materials Research for High Speed Civil Transport and Generic Hypersonics - Adhesive Durability  |   |  | <b>5. FUNDING NUMBERS</b><br>C NAS1-20013<br>Task 11<br>WU 537-06-20-05   |  |
| <b>6. AUTHOR(S)</b><br>Mark R. Allen   |   |  |   |  |
| <b>7. PERFORMING ORGANIZATION NAME(S) AND ADDRESS(ES)</b><br>Boeing Commercial Airplane Group<br>Technology and Product Development<br>P.O. Box 3707<br>Seattle, WA 98124-2207   |   |  | <b>8. PERFORMING ORGANIZATION REPORT NUMBER</b>                           |  |
| <b>9. SPONSORING / MONITORING AGENCY NAME(S) AND ADDRESS(ES)</b><br>National Aeronautics and Space Administration<br>Langley Research center<br>Hampton, VA 236861-0001  |   |  | <b>10. SPONSORING / MONITORING AGENCY REPORT NUMBER</b><br>NASA CR-198193 |  |
| <b>11. SUPPLEMENTARY NOTES</b><br>Langley Technical Monitor: Edward P. Phillips<br>Final Report  |   |  |   |  |
| <b>12a. DISTRIBUTION / AVAILABILITY STATEMENT</b><br>Unclassified - Unlimited<br><br>Subject Category 27   |   |  | <b>12b. DISTRIBUTION CODE</b>   |  |
| <b>13. ABSTRACT (Maximum 200 words)</b><br>This report covers a portion of an ongoing investigation of the durability of adhesives for the High Speed Civil Transport (HSCT) program. Candidate HSCT adhesives need to possess the high-temperature capability required for supersonic flight. This program was designed to initiate an understanding of the behavior of candidate HSCT materials when subjected to combined mechanical and thermal loads. Two adhesives (K3A and FM57) and two adherends (IM7/K3B polymeric composite and the titanium alloy Ti-6Al-4V) were used to fabricate thick adherend lap shear specimens. Due to processing problems, only the FM57/titanium bonds could be fabricated successfully. These are currently undergoing thermo-mechanical fatigue (TMF) testing. There is an acute need for an adhesive to secondarily bond polymeric composite adherends or, alternately polymeric composites that remain stable at the processing temperatures of today's adhesives. |   |  |   |  |
| <b>14. SUBJECT TERMS</b><br>Polymeric composites; Secondary bonding; Thermo-mechanical fatigue (TMF); Primary structural bonding; Long term durability; Candidate HSCT adhesives; Adhesively bonded joints; Thick adherend lap shear specimens; High Speed Civil Transport (HSCT)  |   |  | <b>15. NUMBER OF PAGES</b><br>50  |  |
|  |   |  | <b>16. PRICE CODE</b><br>A03  |  |
| <b>17. SECURITY CLASSIFICATION OF REPORT</b><br>Unclassified   | <b>18. SECURITY CLASSIFICATION OF THIS PAGE</b><br>Unclassified | <b>19. SECURITY CLASSIFICATION OF ABSTRACT</b> | <b>20. LIMITATION OF ABSTRACT</b>   |  |